The Astronomical Journal, 128:1623–1645, 2004 October
© 2004. The American Astronomical Society. All rights reserved. Printed in U.S.A.

THE CHEMICAL PROPERTIES OF MILKY WAY AND M31 GLOBULAR CLUSTERS. I. A COMPARATIVE STUDY

Michael A. Beasley, Jean P. Brodie, and Jay Strader
Lick Observatory, University of California, Santa Cruz, CA 95064; mbeasley@ucolick.org, brodie@ucolick.org, strader@ucolick.org

Duncan A. Forbes and Robert N. Proctor
Centre for Astrophysics and Supercomputing, Swinburne University of Technology, Mail Number 31, P.O. Box 218, Hawthorn, VIC 3122, Australia; dforbes@astro.swin.edu.au, rproctor@astro.swin.edu.au

and

Pauline Barmby and John P. Huchra
Harvard-Smithsonian Center for Astrophysics, 60 Garden Street, Cambridge, MA 02138; pbarmby@cfa.harvard.edu, huchra@cfa.harvard.edu
Received 2004 May 3; accepted 2004 July 8

ABSTRACT

A comparative analysis is performed between high-quality integrated spectral indices of 30 M31 globular clusters, 20 Milky Way globular clusters, and a sample of field and cluster elliptical galaxies. We find that the Lick CN indices in the M31 and Galactic clusters are enhanced relative to the bulges of the Milky Way, M31, and elliptical spheroids, in agreement with Burstein and coworkers. Although not particularly evident in the Lick CN indices, the near-UV cyanogen feature (λ3883) is strongly enhanced with respect to the Galactic globular clusters at metallicities $-1.5 < [\mathrm{Fe/H}] < -0.3$. Carbon shows signs of varying among these two groups. For $[\mathrm{Fe/H}] > -0.8$, we observe no systematic differences in the Hδ, Hγ, or Hβ indices between the M31 and Galactic globular clusters, in contrast to previous studies. The elliptical galaxy sample lies offset from the loci of the globular clusters in both the cyanogen-[MgFe] and Balmer-line–[MgFe] planes. Six of the M31 clusters appear young and are projected onto the M31 disk. Population synthesis models suggest that these are metal-rich clusters with ages 100–800 Myr, metallicities $-0.20 \leq [\mathrm{Fe/H}] \leq 0.35$, and masses $0.7-\sim 7.0 \times 10^4\ M_\odot$. Two other young clusters are Hubble V in NGC 205, observed as a template, and an older ($\sim$3 Gyr) cluster some 7 kpc away from the plane of the disk. The six clusters projected onto the disk show signs of rotation similar to the H I gas in M31, and three clusters exhibit thin disk kinematics, according to Morrison and coworkers. Dynamical mass estimates and detailed structural parameters are required for these objects to determine whether they are massive open clusters or globular clusters. If they are the latter, our findings suggest globular clusters may trace the buildup of galaxy disks. In either case, we conclude that these clusters are part of a young, metal-rich disk cluster system in M31, possibly as young as 1 Gyr old.

Key words: galaxies: individual (M31) — globular clusters: general

1. INTRODUCTION

Understanding the formation and evolution of disk galaxies is a crucial aspect of galaxy formation studies (Freeman & Bland-Hawthorn 2002). Much of our knowledge about such disks is based on detailed observations of the Milky Way, and in this regard its globular clusters (GCs) have played a prominent role. The Milky Way possesses a retinue of $\sim$150 GCs, which, while a minor contributor to the total mass budget of the Galaxy (they constitute some $\sim 3 \times 10^7\ M_\odot$ in total, or $\sim$0.1% of the baryonic mass of the Milky Way), have proved invaluable for understanding its structure, stellar populations, and mass aggregation history (e.g., Searle & Zinn 1978). They are composed of at least two components: a spatially extended, metal-poor, pressure-supported system and a metal-rich, centrally concentrated system that exhibits some rotation (Zinn 1985). Although initially thought to be associated with the thick disk (Zinn 1985), the majority of these metal-rich clusters are now believed to be associated with the bulge (Frenk & White 1982; Minitti 1995; Côté 1999; Forbes et al. 2001).

To date, all the GCs in the Galaxy for which detailed color-magnitude diagrams have been obtained appear "old" (i.e., older than 8 Gyr), although a subset of metal-rich GCs may be up to $\sim$20% younger than the inner halo GCs (Rosenberg et al. 1999; Salaris & Weiss 2002). There is also evidence for a spread of ages among the outer halo GCs, suggesting an origin in either a clumpy collapse (Searle & Zinn 1978) or accretion (e.g., Côté et al. 2000a; Bellazzini et al. 2003). The significance of such accretions is currently the subject of much debate in light of the presently favored hierarchical clustering paradigm (Brook et al. 2003; Martin et al. 2004; Forbes et al. 2004).

Notwithstanding our increasingly detailed knowledge regarding the Milky Way GC system, surprisingly little is known about the GC systems of spiral galaxies in general. This is largely a result of the difficulties involved in observing systems that have few GCs (compared with elliptical galaxies) that are often projected against an inhomogeneous background. However, the gaps in our knowledge about the GC systems of external spiral galaxies are slowly changing with increasingly detailed photometric (e.g., Goudfrooij et al. 2003; Rhode 2003; Chandar et al. 2004) and spectroscopic studies (Chandar et al. 1999; Schroder et al. 2002; Olsen et al. 2004).

In this regard, our close companion, the Andromeda spiral galaxy (M31; $D \sim 780$ kpc, Holland 1998; Stanek & Garnavich 1998) provides an important test bed for the generality of any Milky Way formation theories. It is of similar Hubble type (Sb) to the Milky Way, although it is possibly less massive (Côté et al. 2000b; Gottesman et al. 2002). Unlike the Milky Way, M31 appears to have a predominantly metal-rich stellar halo (e.g., Holland et al. 1996; Bellazzini et al. 2003; Rich et al. 2004).

M31 possesses the most populous GC system in the Local Group. Van den Bergh (1999) estimated a total GC system of 400 ± 55, which is at least a factor of 2 larger than that of the Milky Way. Previous studies to catalog the M31 GC system have included Sargent et al. (1977), Battistini et al. (1980, 1987, 1993), and Crampton et al. (1985). Recently, Barmby et al. (2000) published a comprehensive photometric and spectroscopic catalog of 435 GCs and GC candidates. These authors showed that the M31 GC system could be divided into metal-poor and metal-rich subpopulations, with their kinematics separating them into halo and bulge/disk components similar to that of the Milky Way. Perrett et al. (2002) obtained intermediate-resolution spectra for a subset of $\sim$200 M31 clusters, offering a great improvement in velocity accuracy over previous efforts. This increase in accuracy led a recent study by Morrison et al. (2004) to kinematically identify what is possibly a *thin* disk population of M31 GCs. Such a system has not been observed in the Milky Way.

Van den Bergh (1969) was the first to study the metallicity distributions of GCs in M31 from integrated spectra and *UBV* photometry obtained with the Hale 200 inch (5 m) telescope. He concluded that on average, the M31 GC system was more metal-rich than both the Milky Way and Fornax dwarf GC systems. In an important contribution, Burstein et al. (1984) comprehensively discussed differences in the stellar content of GCs in the Milky Way and M31. From integrated spectra, they found that at high metallicity and at a given metal-line strength, the hydrogen lines (specifically Hβ) of the M31 GCs were systematically stronger than their Galactic counterparts. They explored a number of possible explanations for this phenomenon and concluded that the most likely explanation was an age difference in the GCs, in that the M31 GCs were systematically younger than the Milky Way's. They also found that CN in the intermediate–to–metal-rich M31 GCs was significantly enhanced (by several tenths of a magnitude) when compared to elliptical galaxies. This CN enhancement could not be demonstrated at low metallicities. No satisfactory explanation that could explain both the "CN" anomaly and the enhanced Balmer indices has been put forward.

In a series of papers Brodie & Huchra (1990, 1991; Huchra et al. 1991) investigated the metallicity and abundances of M31 GCs using a more extensive sample of integrated spectra. In general, they found that the properties of the M31 GC system were similar to those of the Galactic system. Notable exceptions were that the CN and H and K line strengths were higher in the M31 GCs (at a given metallicity) than the Galactic GCs, supporting the Burstein et al. (1984) findings. However, with the exception of a few individual cases, they saw no systematic evidence for an enhancement in Hβ in M31 GCs.

The CN enhancement in the M31 GCs is now reasonably well established (Tripicco 1989; Ponder et al. 1998; Li & Burstein 2003), whereas the differences in Hβ are somewhat more controversial (see Tripicco 1993 for a short review). However, it is important to note that in the above studies, the most metal-rich Galactic GCs were not well represented, mostly because of the difficulty of observing these objects against the bright background presented by the Galaxy. If metal-rich GCs are associated with spiral bulges (Frenk & White 1982; Côté 1999; Forbes et al. 2001), then M31's bulge, which is an order of magnitude more massive than that of the Milky Way, should host many more metal-rich bulge GCs, resulting in an unequal comparison between the two GC populations (see Trager 2004).

In this paper, we compare Galactic GC data, which include a number of "bulge GCs" (Cohen et al. 1998; Puzia et al. 2002) and newly analyzed spectroscopic data for M31 GCs in order to investigate some of these issues in detail. In a forthcoming paper (Beasley et al. 2004b, hereafter Paper II), we compare these full data sets to contemporary stellar population models in order to derive parameters such as metallicity, age, and α-to-iron abundance ratios.

The outline of this paper is as follows. In § 2 we discuss the samples under study and new data reduction steps required. Next, details of the spectroscopic system are given in § 3. In § 4 we look at the behavior of the Balmer and CN indices of the GCs as compared to recent elliptical galaxy data. In § 5 we look in detail at eight young clusters in the M31 spectroscopic sample. Finally, we present our discussion and conclusions in § 6.

2. GLOBULAR CLUSTER DATA

2.1. *M31 Globular Clusters*

The integrated spectra of M31 globular clusters used in this study were previously described in Barmby et al. (2000). These authors obtained radial velocities for the clusters and derived metallicities using the empirical calibrations of Brodie & Huchra (1990). We have not used the MMT spectra described in Barmby et al. (2000), since these spectra are generally of insufficient signal-to-noise ratio (S/N) for accurate line-strength analysis. In the following, we describe this data set and outline the data reduction steps that differ from Barmby et al. (2000).

Integrated spectra for 42 GC candidates in M31 were obtained with the Low Resolution Imaging Spectrograph (LRIS; Oke et al. 1995) on the Keck I telescope. The observations were undertaken on 1995 September 21–23 and 1996 December 8, with some effort to obtain spectra of clusters in the central galactic regions of M31. Candidates were drawn from the catalog of Barmby et al. (2000), with the majority originating from the work of Battistini et al. (1987). Integrations were typically 5 minutes per target, which with characteristic magnitudes of $V \sim 17$ yielded spectra with S/N of 20–200 per resolution element. Typical seeing was 1″ during these observations, and the same $1'' \times 1\farcs5$ long slit was used for all clusters. A 600 line mm^{-1} grating was used, yielding a 1.2 Å pixel^{-1} dispersion and a full width at half-maximum resolution (FWHM) of 5 Å. This resolution was determined from measuring a series of isolated arc lines in the comparison lamp spectra and found to be constant over our spectral range 3670–6200 Å.

The data reduction steps of bias subtraction, flat-fielding, and sky subtraction were performed using standard packages in IRAF.[1] The spectra were wavelength-calibrated using arc

[1] IRAF is distributed by the National Optical Astronomy Observatory, which is operated by the Association of Universities for Research in Astronomy, Inc., under cooperative agreement with the National Science Foundation.

TABLE 1
Basic Data for M31 Globular Clusters

Name[a]	R.A.[b] (J2000.0)	Decl.[b] (J2000.0)	X^b (arcmin)	Y^b (arcmin)	Z^b (arcmin)	Velocity[b] (km s^{-1})	S/N[c] (pixel^{-1})	Notes
126-184	0 42 43.78	41 12 42.98	−2.8	−2.0	3.5	−182 ± 14	73	
134-190	0 42 51.72	41 14 02.88	−0.8	−2.4	2.5	−401 ± 32	70	
158-213	0 43 14.47	41 07 20.58	−3.4	−9.9	10.5	−187 ± 6[d]	120	Velocity standard
163-217	0 43 17.71	41 27 45.53	13.0	2.2	13.2	−161 ± 4[d]	170	Velocity standard
222-277	0 44 25.51	41 14 12.62	10.2	−16.2	19.1	−282 ± 20	30	F-type spectrum, peculiar
225-280	0 44 29.78	41 21 36.57	16.5	−12.2	20.5	−167 ± 8[d]	169	Velocity standard
234-290	0 44 46.50	41 29 18.34	24.5	−9.9	26.4	−234 ± 16	71	
292-010	0 36 16.69	40 58 26.64	−58.5	47.1	75.1	−331 ± 23	32	Late F spectrum
301-022	0 38 21.61	40 03 37.22	−87.8	−5.0	88.0	−30 ± 20	31	
304-028	0 38 56.82	41 10 28.81	−30.7	30.3	43.1	−353 ± 15	34	
310-032	0 39 25.82	41 23 33.46	−17.0	34.0	38.0	−189 ± 18	35	
313-036	0 39 44.52	40 52 56.24	−39.1	12.5	41.1	−446 ± 6	52	
314-037	0 39 44.60	40 14 08.23	−69.9	−11.2	70.7	−318 ± 66	17	F0 spectrum
321-046	0 40 15.30	40 27 46.86	−55.5	−7.5	56.0	−527 ± 35	30	A-type spectrum
322-049	0 40 17.28	40 39 05.83	−46.3	−0.8	46.3	−581 ± 29	40	A-type spectrum
324-051	0 40 20.75	41 40 50.79	3.0	36.4	36.5	−299 ± 35	69	F-type spectrum, Hubble V
327-053	0 40 24.09	40 36 22.75	−47.7	−3.5	47.8	−658 ± 29	71	A–F spectrum
328-054	0 40 24.86	41 40 23.74	3.1	35.5	35.6	−243 ± 23	30	
337-068	0 40 48.45	42 12 10.45	30.9	51.5	60.0	50 ± 12	178	CN weak, CH strong?
347-154	0 42 22.95	41 54 28.25	27.7	26.7	38.5	−312 ± 36	61	
350-162	0 42 28.43	40 24 52.18	−42.2	−29.2	51.4	−457 ± 18	39	
365-284	0 44 36.77	42 17 20.47	61.0	21.4	64.7	−78 ± 13	60	
380-313	0 46 06.34	42 00 53.23	58.5	−1.9	58.5	−121 ± 31	43	F0 spectrum
383-318	0 46 11.89	41 19 42.15	27.0	−28.4	39.1	−250 ± 10	85	
393-330	0 47 01.22	41 24 06.45	36.2	−32.8	48.9	−331 ± 10	43	
398-341	0 47 57.83	41 48 44.63	62.0	−25.6	67.1	−227 ± 5	44	
401-344	0 48 08.52	41 40 42.47	57.0	−32.2	65.5	−273 ± 52	54	
NB 16	0 42 33.18	41 20 17.12	2.0	4.2	4.6	−115 ± 15	142	
NB 67	0 42 34.18	41 19 47.10	1.7	3.7	4.1	−113 ± 17	91	
NB 89	0 42 44.69	41 14 41.97	−1.1	−1.0	1.5	−332 ± 6	110	

Notes.—Units of right ascension are hours, minutes, and seconds, and units of declination are degrees, arcminutes, and arcseconds. The values X, Y, and Z are defined in Huchra et al. (1991).
[a] Nomenclature from Huchra et al. (1991).
[b] Data from Barmby et al. (2000).
[c] Derived S/N measured at 5000 Å.
[d] Echelle velocities from Peterson (1989).

lamp spectra, covering the full spectral range, which were interspersed among the M31 observations.

The accuracy of the relative flux calibrations of the spectra can have a significant impact on the measurement of certain broad line-strength indices. For these data, this is true of the Lick CN_1, CN_2, Mg_1, Mg_2, and TiO_1 indices. For the present study, the original non–flux-calibrated spectra from Barmby et al. (2000) have been re-fluxed using a larger series of flux standards taken during the time of the LRIS observations. These flux standards, BD +28°4211, BD +25°4655, Feige 110, and GD 50, were all selected from the faint spectrophotometric standard star list of Oke (1990). The standards were all taken with the same slit size ($1'' \times 1'.5$) as the program observations and covered a range of air masses. In general, the new flux calibrations agree to within ∼10% of the old calibrations. However, we do observe significant differences in the spectra that exhibit earlier spectral types (see § 5), which we attribute to differences in air mass between the original flux standards and the program clusters. The following analysis is based on the newly flux-calibrated M31 data.

Reliable line-strength measurements require a S/N such that the index and pseudocontinuum are well defined. Therefore, we have focused on a high-S/N (>30 pixel^{-1}) subset of these data. From 42 spectra of candidate M31 GCs, 36 are of sufficient S/N for a detailed analysis of their line-strength indices. Five clusters, all drawn from the near-nucleus cluster catalog of Battistini et al. (1993), have been identified as being likely foreground G dwarfs on the basis of their spectra. These objects exhibit weak CN and TiO molecular bands, closely following the dwarf sequences of the Lick stellar library rather than that of the majority of the M31 GCs and Lick giants. Moreover, a measure of their surface gravities based on the Sr II/Fe I diagnostic (Rose 1985) places them clearly on the locus of Lick dwarfs rather than that of a dwarf-giant mix expected for GCs (Tripicco 1989).[2] These objects (NB 68, 74, 81, 87, and 91) were removed from the sample. The basic data for all the M31 clusters that satisfy our S/N and "star cluster" criteria are listed in Table 1. The spatial distribution of the sample with respect to M31 is shown in Figure 1.

To anticipate some of the results of this study, spectra for eight of the M31 GC candidates have spectral characteristics typical of young stellar populations or A–F stars: weak metal

[2] Although circumstantial, these clusters also possess a mean velocity of −93 km^{-1}. This places them at the lower velocity end of the M31 GC velocity distribution, which has a maximum-likelihood systemic velocity of −284 ± 9 km s^{-1} and an overall velocity dispersion of 156 ± 6 km s^{-1} (Perrett et al. 2002).

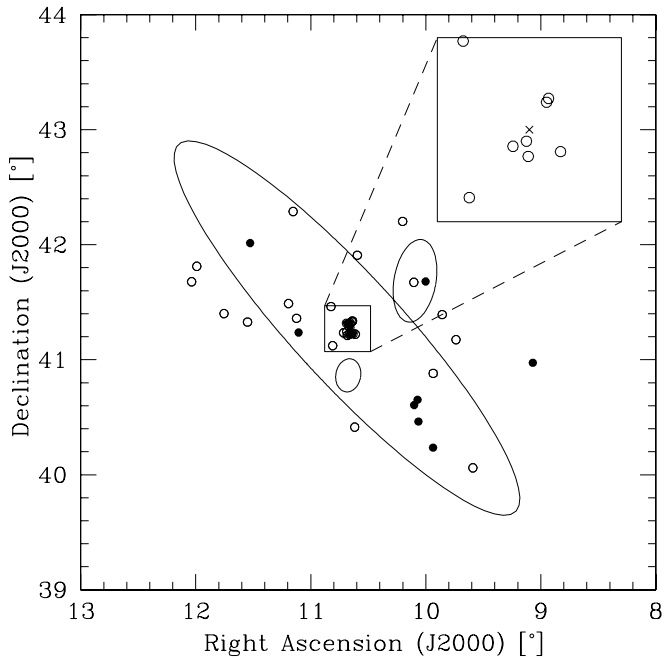

FIG. 1.—Spatial distribution of sample GCs in M31. Open circles represent "normal" GCs and filled circles represent clusters that we identify as young (less than a few gigayears). Ellipses represent faint isophotes of M31, M32 (*lower left*), and NGC 205 (*upper right*). Most GCs have a projected location in the disk/halo of M31; however, several are concentrated in the galactic central regions, which are shown in the enlargement in the upper right corner.

lines, relatively strong absorption in the hydrogen Balmer lines, and relatively blue continua when compared to "classical" G- or K-type GC spectra. These are discussed separately in § 5 and are not included in the main analysis.

2.2. *Galactic Globular Clusters*

Galactic GCs play a vital role in the interpretation of the integrated light of more distant GC systems. They not only allow for direct comparative studies but also provide important benchmarks for stellar population models, since they generally have independently derived ages, metallicities, and often heavy-element abundance ratios. Increasingly, high-quality integrated spectra for Galactic GCs are appearing in the literature, and we make use of two such studies.

Cohen et al. (1998, hereafter CBR98) obtained LRIS long-slit spectra for 12 Galactic GCs in order to compare with their multislit M87 GC data. These spectra were obtained by scanning ~90″ across the cores of the Galactic GCs in order to synthesize a larger aperture and thus obtain a representative integrated spectrum. These data are all of high S/N but were taken using differing grating angles, yielding six spectra with wavelength ranges in the interval 3800–6500 Å and six spectra slightly shifted to the red with wavelength ranges of 4500–7200 Å. The LRIS 600 lines mm^{-1} grating used yielded a dispersion of 1.2 Å pixel^{-1} and resolution (FWHM) of ~6 Å.

CBR98 did not flux-calibrate these data and measured indices by individually shifting each index to its rest wavelength. We elected to derive new wavelength solutions for the 12 spectra (kindly provided by J. Cohen and J. Blakeslee; see Beasley et al. 2004a) by comparing the central index positions in these spectra with known wavelengths from our present M31 data and Galactic GC data from Puzia et al. (2002). We have also performed a first-order flux calibration to the spectra using the sensitivity functions derived from our long-slit LRIS data using a similar instrumental setup.[3]

Puzia et al. (2002, hereafter P02) have presented high-quality integrated spectra for 12 Galactic GCs, with the inclusion of a number of bulge clusters. Their sample also contains an integrated spectrum of the outer bulge of the Galaxy. These authors obtained fixed-position (i.e., not drift-scanned) spectra with different pointings (see P02) using the Boller and Chivens Spectrograph at the ESO 1.52 m telescope at La Silla. A 600 line mm^{-1} grating gave 1.89 Å pixel^{-1}, with a fixed 3″ slit yielding a resolution of ~6.7 Å.

Four of the GCs in the P02 sample are in common with those in the CBR98 sample, namely, NGC 6356, 6528, 6553, and 6624, resulting in a total of 20 unique GCs for our analysis. These four common clusters between the CBR98 and P02 data sets have allowed us to examine any systematic offsets between these data, in addition to estimating the true uncertainties in the CBR98 data (§ 3).

3. LINE-STRENGTH INDICES

3.1. *Lick Indices*

We have chosen to investigate the chemical properties of the M31 and Galactic globular clusters using the line-strength indices defined by the Lick group (Burstein et al. 1984; Trager et al. 1998). For the following discussion, we first draw a clear distinction between the Lick *indices* and the Lick *system*.

Lick indices now describe a set of 25 indices (see Trager et al. 1998 and Worthey & Ottaviani 1997 for the latest definitions) that are defined by two central feature bandpasses and four pseudocontinuum bandpasses (a total of six bandpasses or wavelengths). However, the Lick system refers to Lick indices that are measured on spectra that match (or mimic) the behavior of the mildly nonlinear and non–flux-calibrated Lick/Image Dissector Scanner (Lick/IDS). This is achieved by virtue of either the spectra having been acquired with the Lick/IDS or by calibrating onto the Lick/IDS system by matching its resolution and correcting for systematic offsets through observing sufficient Lick standard stars.

The advantages in using the Lick system and indices are that they are widely used by Galactic and GC researchers and that an extensive stellar library exists for the construction of stellar population models (e.g., Worthey et al. 1994). Important drawbacks are that calibrating non-Lick/IDS data onto the Lick system can be difficult, generally requiring many observations of standard stars, and that data of higher resolution than that of the Lick library (8–11 Å) must be degraded to this resolution, potentially losing important information.

In principle, line-strength indices measured on flux-calibrated spectra obtained with modern spectrographs and linear detectors should be well reproducible, provided these data are at the same resolution (e.g., Vazdekis 1999). For the case of spectra with good sky subtraction and flat-fielding, no systematic offsets should be observed between measurements of common objects, with the scatter entirely reflecting the random uncertainties between the two observations. Therefore, we have chosen not to correct these data to the Lick system but to compare the CBR98, M31, and P02 data at the Lick resolution. Note that for the P02 data, we have "de-Licked" these indices using the values given in P02. However, for

[3] In the case of the CBR98 data, we found that the effect on the measured line strengths using flux- versus non–flux-calibrated spectra was within the measurement uncertainties even for broad indices.

comparison with stellar population models based on the Worthey et al. (1994) Lick fitting functions, correction to the Lick system is a requirement. We determine these corrections in § 3.2.

To match the Lick/IDS resolution, the CBR98 and M31 data have been smoothed with a wavelength-dependent Gaussian kernel based on the known variation of FWHM with wavelength of the Lick/IDS given in Worthey & Ottaviani (1997). These M31 data were then shifted to the rest frame using the velocities given in Barmby et al. (2000). This shift was unnecessary for the CBR98 data, since they were wavelength-calibrated in the rest frame (§ 2.2).

CBR98 originally measured a subset of Lick indices from their spectra using the original index definitions of Burstein et al. (1984). For these recalibrated CBR98 data, we have measured Lick indices using the updated definitions in Trager et al. (1998) and Worthey & Ottaviani (1997). Note that the differing grating angles used in these observations (§ 2.2) yielded different spectral ranges, resulting in six clusters that do not have measured indices blueward of 4500 Å ($C_2$4668). All the measured Lick indices that fall within the spectral range are given in Table 2.

Due to the high-S/N nature of these spectra, photon statistical errors generally underestimate the real uncertainty in the Lick indices measured. Since we have no repeat observations of these clusters with which to determine our repeatability, we have estimated the uncertainty in each index by comparing our measured Lick indices with four GCs that are in common with the P02 sample. We determine the rms difference between each Lick index to yield $\sigma_{\rm rms}$.[4] The mean difference and $\sigma_{\rm rms}$ for each index between the common clusters are listed in Table 3. Unfortunately, only one of the Galactic clusters common to the CBR98 and P02 data sets (NGC 6356) includes all the blue indices in the CBR98 spectrum. Therefore, $\sigma_{\rm rms}$ for indices Hδ_F to Fe4531 was taken to be the absolute difference between the measurements. The shot-noise uncertainties for these data were determined using the method described by Cardiel et al. (1998), which we denote σ_S, yielding a total error $\sigma_T^2 = \sigma_{\rm rms}^2 + \sigma_S^2$. Values of σ_T are also given in alternate rows in Table 2.

As can be seen, in general the agreement between the two data sets is good, and offsets between the CBR98 and P02 data are small. This is true for the most important indices (e.g., CN, Mg_2, Mg *b*, Fe5270, and Fe5335). We see significant offsets in G4300, Hγ_A, $C_2$4668, and Fe5015. The reason for these differences is unclear; however, we note that the Lick corrections employed by P02 for these indices (by which we have decorrected these indices) are significant.

For the M31 data, 24 Lick indices were measured from Hδ_A (the bluest) to TiO_1 (the reddest) as defined in Trager et al. (1998) and Worthey & Ottaviani (1997). We were unable to measure TiO_2, since this index extends beyond our red wavelength limit. These indices are tabulated in Tables 4A and 4B. We have estimated the uncertainties in these data by comparing clusters in common between the two observing runs. There are three clusters in common, which are commonly used as velocity standards: 158-213, 163-217, and 225-280 (using the nomenclature of Huchra et al. 1991), and we have taken the rms, $\sigma_{\rm rms}$, between index measurements of these clusters as an estimate of our repeatability.

[4] In principle, this actually provides an overestimation, since we also include the intrinsic uncertainties within the P02 data. However, the quadrature subtraction of these uncertainties in some cases leads to an uncertainty of zero.

This method worked well for most indices, and any systematic offsets were generally small. The exceptions to this were Hδ_A and Na D, both of which showed rather large offsets between the 1995 December and 1996 September runs (−0.4 and −0.5 Å, respectively) for reasons that remain unclear. In view of this we assigned rms values of 0.4 and 0.5 Å, respectively, and note that these are problematic indices. Poisson (shot-noise) errors (σ_S) were calculated as for the CBR98 data. Values of σ_T are given in alternate rows in Tables 4A and 4B.

3.2. *Corrections to the Lick/IDS System*

The usual method for correcting to the Lick/IDS system is to observe a range of standard stars in the Lick library that cover the metallicities and range of spectral types of the stellar populations under study (González 1993). Ideally, these stellar spectra should be obtained at the same time as the program observations and, crucially, obtained using the same instrumental setup. Comparison with the Lick/IDS tabulated values then provides the required corrections (linear or otherwise) in order to mimic the Lick/IDS system.

Unfortunately, no such observations were taken for the CBR98 data nor for the M31 data. However, there are six Galactic GCs in common between the CBR98 data and Trager et al. (1998), and there are three M31 GCs in common between the M31 and Trager et al. (1998) data. The six clusters in common between the CBR98 data and Trager et al. (1998) are NGC 6171, 6205 (M13), 6341 (M92), 6356, 6624, and 6838 (M71). Trager et al. (1998) did not measure the higher order Balmer lines (Hδ, Hγ) for these data, and therefore we have taken the indices measured on the Lick/IDS spectra from Kuntschner et al. (2002). Note that the Galactic and M31 cluster indices given in Trager et al. (1998) were first published in Burstein et al. (1984), with the older Lick indices given in this paper. In order to be consistent with the index bandpass definitions in this study, all our comparisons are performed against the newer measurements given in Trager et al. (1998).

To characterize the relationships between the Lick and CBR98 index measurements, we have used a simple least-squares linear fit, $I_{\rm Lick} = a + bI_{\rm CBR98}$, where $I_{\rm Lick}$ and $I_{\rm CBR98}$ are the indices in question measured on the Lick and CBR98 data and the coefficients *a* and *b* are given in Table 5, along with the rms of the least-squares fit. We have also calculated the mean difference between these observations (Lick minus CBR98) and their respective standard deviations, which provide first-order corrections (i.e., additive corrections), and tabulate them in Table 5. For several of the indices (G4300, Fe4383, Fe4531, $C_2$4668, and Fe5709) NGC 6171 showed large deviations from the mean, and these were removed from our calculations. We were unable to obtain any corrections for the bluest Lick index Hδ_A.

Comparison between the Trager et al. (1998) and CBR98 data shows significant deviations from unit slope for some indices (Table 5). In some cases, this may be attributable to resolution differences between the spectra (e.g., P02). We tested this by broadening the CBR98 data with wavelength-dependent Gaussian kernels several angstroms (FWHM) higher and lower than that of the Lick/IDS resolution and remeasuring Lick indices. In general, we found that we could induce changes in slope of no more than 10% in these indices with the exceptions of Ca4227 and Fe5335, which are known to be very sensitive to resolution (Vazdekis 1999).

TABLE 2

Lick/IDS Indices and Uncertainties Measured for the Galactic GCs in the Cohen et al. (1998) Sample

Name	$H\delta_A$ (Å)	$H\delta_F$ (Å)	CN_1 (mag)	CN_2 (mag)	Ca4227 (Å)	G4300 (Å)	$H\gamma_A$ (Å)	$H\gamma_F$ (Å)	Fe4384 (Å)	Ca4455 (Å)	Fe4531 (Å)	$C_2$4668 (Å)
NGC 6205.....	...	...	...	...	0.32	2.14	1.54	1.90	0.86	0.11	1.10	0.19
	...	...	...	...	±0.03	±0.57	±0.54	±0.17	±0.34	±0.05	±0.07	±0.46
NGC 6121.....	...	...	...	...	0.40	2.72	1.58	2.23	1.76	0.22	1.48	0.62
	...	...	...	...	±0.05	±0.58	±0.55	±0.18	±0.35	±0.07	±0.10	±0.47
NGC 6838.....	...	−0.34	0.005	0.023	0.81	5.30	−4.57	−1.11	3.13	0.57	2.55	2.10
	...	±0.12	±0.003	±0.003	±0.03	±0.57	±0.54	±0.17	±0.34	±0.04	±0.06	±0.46
NGC 6341.....	...	...	...	...	0.17	1.04	2.78	2.44	0.61	0.09	0.57	0.08
	...	...	...	...	±0.03	±0.57	±0.54	±0.17	±0.34	±0.04	±0.07	±0.46
NGC 6171.....	...	...	...	...	...	−0.47	4.96	2.52	1.48	0.14	−0.51	0.32
	...	...	...	...	...	±0.61	±0.57	±0.21	±0.46	±0.16	±0.23	±0.54
NGC 6356.....	...	0.60	0.044	0.067	0.75	4.97	−3.81	−0.60	3.25	0.69	2.62	2.06
	...	±0.13	±0.003	±0.003	±0.04	±0.57	±0.55	±0.18	±0.34	±0.05	±0.08	±0.46
NGC 6440.....	...	...	...	...	...	...	...	...	...	...	...	2.42
	...	...	...	...	...	...	...	...	...	...	...	±0.46
NGC 6528.....	...	...	...	...	...	...	...	...	...	...	...	3.88
	...	...	...	...	...	...	...	...	...	...	...	±0.47
NGC 6539.....	...	...	...	...	...	...	...	...	...	...	...	2.68
	...	...	...	...	...	...	...	...	...	...	...	±0.51
NGC 6553.....	...	...	...	...	...	...	...	...	...	...	...	3.92
	...	...	...	...	...	...	...	...	...	...	...	±0.46
NGC 6624.....	...	...	...	...	...	...	...	...	...	...	...	1.83
	...	...	...	...	...	...	...	...	...	...	...	±0.45
NGC 6760.....	...	...	...	...	...	...	...	...	...	...	...	2.15
	...	...	...	...	...	...	...	...	...	...	...	±0.47

Name	$H\beta$ (Å)	Fe5015 (Å)	Mg_1 (mag)	Mg_2 (mag)	Mg *b* (Å)	Fe5270 (Å)	Fe5335 (Å)	Fe5406 (Å)	Fe5709 (Å)	Fe5782 (Å)	Na D (Å)	TiO_1 (mag)
NGC 6205.....	2.47	1.43	0.008	0.048	0.83	0.87	0.74	0.38	0.23	0.11	0.91	0.003
	±0.13	±0.23	±0.014	±0.010	±0.08	±0.14	±0.13	±0.17	±0.11	±0.13	±0.10	±0.012
NGC 6121.....	2.91	2.26	0.031	0.094	1.57	1.26	0.96	0.51	0.47	0.36	1.68	0.009
	±0.13	±0.24	±0.014	±0.010	±0.08	±0.14	±0.13	±0.17	±0.11	±0.13	±0.10	±0.012
NGC 6838.....	1.43	3.79	0.074	0.164	2.71	2.17	1.95	1.32	0.78	0.57	2.28	0.023
	±0.13	±0.22	±0.014	±0.010	±0.08	±0.13	±0.13	±0.17	±0.11	±0.13	±0.10	±0.012
NGC 6341.....	2.55	0.66	0.004	0.029	0.52	0.48	0.43	0.18	0.09	0.04	0.68	0.003
	±0.13	±0.23	±0.014	±0.010	±0.08	±0.13	±0.13	±0.17	±0.11	±0.13	±0.10	±0.012
NGC 6171.....	1.60	2.53	0.041	0.118	1.81	1.50	1.21	0.68	0.49	0.47	1.86	0.017
	±0.16	±0.30	±0.014	±0.010	±0.12	±0.17	±0.17	±0.19	±0.12	±0.14	±0.12	±0.012
NGC 6356.....	1.63	3.57	0.072	0.172	3.02	2.01	1.84	1.21	0.79	0.65	3.05	0.030
	±0.13	±0.23	±0.014	±0.010	±0.08	±0.14	±0.13	±0.17	±0.11	±0.13	±0.10	±0.012
NGC 6440.....	1.44	3.90	0.102	0.225	3.25	2.32	1.73	1.19	0.90	1.02	4.21	0.030
	±0.13	±0.23	±0.014	±0.010	±0.08	±0.13	±0.13	±0.17	±0.11	±0.12	±0.10	±0.012
NGC 6528.....	1.83	5.00	0.097	0.246	3.81	2.79	2.21	1.62	1.05	1.00	5.12	0.044
	±0.13	±0.23	±0.014	±0.010	±0.08	±0.14	±0.13	±0.17	±0.11	±0.13	±0.10	±0.012
NGC 6539.....	1.40	3.94	0.084	0.193	2.81	2.14	1.54	1.19	0.92	0.96	4.05	0.037
	±0.15	±0.27	±0.014	±0.010	±0.10	±0.15	±0.15	±0.18	±0.11	±0.13	±0.11	±0.012
NGC 6553.....	1.68	5.08	0.106	0.262	3.99	2.96	2.36	1.67	0.97	1.09	3.70	0.048
	±0.13	±0.22	±0.014	±0.010	±0.08	±0.13	±0.13	±0.17	±0.11	±0.12	±0.10	±0.012
NGC 6624.....	1.71	3.61	0.048	0.161	2.83	1.93	1.59	1.07	0.65	0.57	2.47	0.031
	±0.13	±0.22	±0.014	±0.010	±0.07	±0.13	±0.12	±0.17	±0.10	±0.12	±0.10	±0.012
NGC 6760.....	1.38	4.11	0.095	0.225	3.30	2.30	1.78	1.29	0.83	0.87	3.51	0.045
	±0.13	±0.23	±0.014	±0.010	±0.08	±0.14	±0.13	±0.17	±0.11	±0.13	±0.10	±0.012

TABLE 3
MEAN OFFSETS AND STANDARD DEVIATIONS BETWEEN P02 AND CBR98 INDICES

Index	P02 minus CBR98	σ_{rms}
$H\delta_A$	...	...
$H\delta_F$	0.1144	0.1144[a]
CN_1	0.0027	0.0027[a]
CN_2	0.0018	0.0018[a]
Ca4227	0.0044	0.0044[a]
G4300	−0.5746	0.5746[a]
$H\gamma_A$	−0.5411	0.5411[a]
$H\gamma_F$	−0.1702	0.1702[a]
Fe4383	−0.3277	0.3277[a]
Ca4455	0.0042	0.0042[a]
Fe4531	0.0299	0.0299[a]
$C_2$4668	0.5646	0.4533
$H\beta$	−0.0027	0.1257
Fe5015	−0.8856	0.2142
Mg_1	−0.0087	0.0136
Mg_2	−0.0043	0.0096
Mg *b*	−0.1616	0.0723
Fe5270	0.0650	0.1309
Fe5335	0.0025	0.1199
Fe5406	−0.1590	0.1689
Fe5709	0.3026	0.1036
Fe5782	0.0063	0.1235
Na D	−0.1975	0.0979
TiO_1	0.0076	0.0115
TiO_2	0.0228	0.0123

NOTE.—Indices at the Lick/IDS resolution, but uncalibrated to the Lick system.
[a] Value of σ_{rms} taken to be the absolute difference.

For the M31 data, there are three clusters that are in common with the Trager et al. (1998) sample. This is not sufficient to securely characterize any changes in slope. However, these three clusters (158-213, 163-217, and 255-280) do populate a reasonable range over the metallicity distribution of M31 clusters (Brodie et al. give metallicities for these clusters of $[Fe/H] = -1.08 \pm 0.05$,[5] -0.36 ± 0.27, and -0.70 ± 0.12, respectively). Moreover, these three clusters are among the highest S/N spectra in our M31 sample. In general the agreement between the M31 and Trager et al. (1998) indices is encouraging. We list the linear fit coefficients *a*, *b*, the rms of the fit, the mean values of (Lick minus M31), and the standard deviations for each index in Table 6.

4. ANALYSIS OF THE MAIN SAMPLE

For the remainder of this paper, we use the indices given in Tables 2, 4A, and 4B, uncorrected to the Lick system. Where there are clusters common between the CBR98 and P02 Galactic data, we have used the P02 data because of their more reliable error estimates.

4.1. *Balmer Lines*

Spinrad & Schweizer (1972), Rabin (1981), and later Burstein et al. (1984) found evidence that M31 GCs were enhanced in the Balmer lines with respect to their Galactic counterparts.[6] Specifically, Burstein et al. (1984) found that at a given Mg_2 line strength, the $H\beta$ index was on average higher than that of the Galactic GCs at $Mg_2 > 0.1$. These authors explored three possible origins for these differences—contributions from hot horizontal-branch stars, blue stragglers, or younger ages—and favored the third interpretation.

Subsequent work by Brodie & Huchra (1990, 1991) and Huchra et al. (1991) with a more extensive sample indicated that only a subset of M31 clusters appeared to have such enhanced $H\beta$, and indeed this question still remains controversial. We now examine this issue with the Galactic and M31 GC data.

In Figure 2 we plot the Lick Balmer indices of CBR98 and P02 compared to the M31 data at a given value of [MgFe].[7] We use [MgFe] since it is metallicity-sensitive, relatively insensitive to abundance ratio variations (González 1993; Thomas et al. 2003), and the narrow indices Mg *b*, Fe5270, and Fe5335 are not particularly susceptible to systematic offsets between data.

The first things to note in the four panels of Figure 2 are the discontinuities in the plots at $[MgFe] \sim 1.6$. These gaps in the index-index relations reflect the well-established bimodality of the Galactic and M31 cluster systems, a gap that is not particularly evident in the Trager et al. (1998) data. The presence of these discontinuities reflects the high S/N of these present data. To contrast the Balmer indices of these data, we find it convenient to separate the clusters into two groups, $[MgFe] < 1.5$ and $[MgFe] \geq 1.5$. Using the empirical [MgFe]-[Fe/H] relation derived by P02, $[MgFe] = 1.5$ Å corresponds to $[Fe/H] \sim -0.8$. We refer to these groups as the "low-metallicity" and "high-metallicity" groups, respectively.

Inspection of Figure 2 shows no evidence of systematic enhancements in $H\beta$, $H\gamma$, or $H\delta$ between the high-metallicity M31 and Galactic GC data. Furthermore, there is no evidence of a significant change in slope in any of the index-index plots that were seen by Burstein et al. (1984). While there does appear to be a mild enhancement in several clusters at $[MgFe] \sim 2$, which is most pronounced in their $H\gamma_A$ and $H\gamma_F$ indices, this is not particularly significant, since there are two Galactic GCs (NGC 6388 and NGC 6637) at this metallicity that differ by ~0.4 Å in $H\beta$; NGC 6388 lies squarely among these M31 clusters. The mean values of the $H\beta$ indices for all the high-metallicity M31 and Galactic clusters (P02 and CBR98 data) are 1.75 ± 0.14 and 1.63 ± 0.20 Å, respectively. The straight mean, however, is not the fairest comparison in this case, since the slope of [MgFe]-$H\beta$ is nonzero and there are relatively more M31 clusters at $[MgFe] \sim 2$ than there are Galactic clusters. The mean $H\beta$ of solely the metal-rich P02 data yields 1.74 ± 0.16 Å, which is identical to that of the metal-rich M31 GCs.

Turning our attention to the metal-poor clusters, the M31 GCs do appear to have somewhat stronger $H\beta$ and $H\gamma_F$ indices. The mean $H\beta$ for these metal-poor M31 clusters is 2.95 ± 0.35 Å, whereas that of the metal-poor Galactic clusters is 2.52 ± 0.22 Å. This difference of 0.43 Å in $H\beta$ is close to the dispersion in the metal-poor M31 clusters alone. Such variations are not particularly unusual among metal-poor GCs and possibly arise from differences in horizontal-branch morphology (Lee et al. 2000; P02).

In Figure 2 we have also plotted the high-quality data for Coma and field elliptical galaxies from Sánchez-Blázquez et al. (2003). Their sample consists of 59 galaxies from the

[5] Unless stated otherwise, [Fe/H] refers to metallicities on the Zinn & West (1984) scale.

[6] Note that although Rabin (1981) and Burstein et al. (1984) reached similar conclusions regarding Balmer line enhancements, in detail their respective $H\beta$ measurements show very poor agreement.

[7] $[Mg\ b \times (Fe\ \lambda5270 + Fe\ \lambda5335)]^{1/2}$; González (1993).

TABLE 4A

LICK/IDS INDICES AND UNCERTAINTIES FOR M31 GLOBULAR CLUSTERS: 4000–4800 Å

Name	$H\delta_A$ (Å)	$H\delta_F$ (Å)	CN_1 (mag)	CN_2 (mag)	Ca4227 (Å)	G4300 (Å)	$H\gamma_A$ (Å)	$H\gamma_F$ (Å)	Fe4384 (Å)	Ca4455 (Å)	Fe4531 (Å)	$C_2$4668 (Å)
126-184	3.82	3.03	−0.060	−0.029	0.42	2.44	1.80	2.77	1.06	0.26	1.43	0.75
	±0.53	±0.47	±0.017	±0.018	±0.17	±0.30	±0.29	±0.17	±0.50	±0.21	±0.31	±0.44
134-190	0.58	0.91	0.010	0.040	0.64	4.53	−2.57	0.34	2.86	0.49	2.38	1.73
	±0.52	±0.47	±0.017	±0.018	±0.17	±0.28	±0.31	±0.19	±0.50	±0.21	±0.31	±0.45
158-213	0.27	1.10	0.040	0.068	0.62	4.06	−2.53	0.18	2.91	0.63	2.40	1.97
	±0.44	±0.38	±0.015	±0.016	±0.09	±0.16	±0.19	±0.12	±0.37	±0.12	±0.19	±0.28
163-217	−0.40	0.68	0.160	0.207	1.03	5.06	−5.26	−1.02	4.52	1.25	3.37	4.06
	±0.43	±0.37	±0.014	±0.015	±0.07	±0.12	±0.16	±0.09	±0.33	±0.09	±0.15	±0.21
222-277	6.98	4.60	−0.120	−0.076	0.72	1.87	4.06	3.57	1.86	0.78	2.74	1.39
	±0.67	±0.62	±0.022	±0.025	±0.31	±0.57	±0.51	±0.31	±0.85	±0.40	±0.59	±0.89
225-280	−0.88	0.64	0.090	0.129	0.78	4.57	−3.71	−0.22	3.82	0.99	2.84	2.95
	±0.43	±0.37	±0.014	±0.015	±0.07	±0.12	±0.16	±0.09	±0.34	±0.09	±0.16	±0.22
234-290	−0.10	0.85	0.000	0.030	0.75	4.37	−3.21	−0.18	2.49	0.52	2.56	1.77
	±0.51	±0.45	±0.016	±0.018	±0.15	±0.26	±0.30	±0.18	±0.48	±0.20	±0.30	±0.44
292-010	4.47	3.39	−0.070	−0.028	0.29	2.45	1.79	2.55	0.82	0.14	0.66	1.23
	±0.64	±0.58	±0.021	±0.023	±0.29	±0.51	±0.50	±0.30	±0.82	±0.39	±0.60	±0.88
301-022	3.60	2.17	−0.080	−0.056	0.89	3.02	0.85	1.91	1.21	0.43	1.73	0.72
	±0.78	±0.76	±0.024	±0.027	±0.35	±0.63	±0.61	±0.38	±0.94	±0.44	±0.65	±0.95
304-028	1.94	2.05	−0.050	−0.019	0.32	2.29	1.13	1.87	0.57	0.23	0.68	−0.18
	±0.69	±0.64	±0.021	±0.024	±0.30	±0.53	±0.51	±0.32	±0.82	±0.39	±0.59	±0.86
310-032	4.07	2.98	−0.110	−0.072	0.44	1.77	1.34	1.85	0.62	0.01	1.26	−0.22
	±0.68	±0.64	±0.021	±0.024	±0.31	±0.55	±0.52	±0.32	±0.84	±0.40	±0.59	±0.86
313-036	0.51	0.96	0.010	0.046	0.75	4.20	−2.75	−0.01	2.53	0.60	2.14	2.09
	±0.56	±0.51	±0.017	±0.019	±0.20	±0.34	±0.37	±0.23	±0.57	±0.25	±0.38	±0.56
314-037	7.85	4.83	−0.170	−0.141	0.94	0.45	6.59	5.07	−0.12	1.31	3.28	1.57
	±0.81	±0.77	±0.028	±0.032	±0.43	±0.87	±0.71	±0.42	±1.29	±0.61	±0.92	±1.45
321-046	10.69	7.55	−0.220	−0.149	0.25	−1.98	9.47	6.97	0.44	0.56	1.00	0.33
	±0.61	±0.54	±0.022	±0.024	±0.32	±0.63	±0.45	±0.26	±0.89	±0.42	±0.66	±0.98
322-049	7.88	5.77	−0.160	−0.106	0.01	−1.68	7.09	5.53	−0.06	0.00	0.93	0.83
	±0.52	±0.46	±0.018	±0.020	±0.21	±0.41	±0.33	±0.19	±0.64	±0.30	±0.46	±0.69
324-051	6.75	4.83	−0.120	−0.069	0.29	0.84	4.89	4.42	0.74	0.36	2.34	2.11
	±0.46	±0.40	±0.016	±0.017	±0.13	±0.24	±0.23	±0.13	±0.45	±0.18	±0.27	±0.42
327-053	5.85	4.40	−0.080	−0.030	0.05	−1.03	5.56	4.58	0.37	0.52	0.72	1.04
	±0.45	±0.39	±0.015	±0.016	±0.12	±0.24	±0.21	±0.12	±0.44	±0.17	±0.28	±0.41
328-054	3.98	2.72	−0.090	−0.057	0.75	2.17	1.51	2.36	0.46	0.32	0.56	−0.22
	±0.70	±0.66	±0.022	±0.025	±0.32	±0.60	±0.57	±0.34	±0.93	±0.44	±0.68	±0.99
337-068	2.66	2.29	−0.060	−0.030	0.60	3.73	−0.02	1.79	2.22	0.58	2.10	1.60
	±0.43	±0.37	±0.015	±0.015	±0.07	±0.13	±0.16	±0.09	±0.34	±0.09	±0.16	±0.22
347-154	4.38	3.12	−0.080	−0.036	0.29	1.24	2.83	2.89	0.52	0.03	1.01	0.51
	±0.51	±0.45	±0.017	±0.018	±0.17	±0.31	±0.29	±0.18	±0.53	±0.22	±0.34	±0.50
350-162	3.50	2.69	−0.050	−0.013	0.35	2.55	1.11	2.12	1.29	0.21	1.20	0.89
	±0.59	±0.54	±0.019	±0.021	±0.25	±0.43	±0.43	±0.26	±0.70	±0.33	±0.50	±0.74
365-284	2.83	2.47	−0.060	−0.025	0.32	2.53	1.33	2.35	1.12	0.33	1.53	0.71
	±0.52	±0.46	±0.017	±0.018	±0.17	±0.30	±0.30	±0.18	±0.53	±0.22	±0.34	±0.50
380-313	9.60	6.46	−0.190	−0.123	0.41	−0.17	8.20	6.32	−0.08	0.37	1.84	0.61
	±0.50	±0.44	±0.017	±0.019	±0.19	±0.38	±0.31	±0.17	±0.61	±0.27	±0.41	±0.63
383-318	−0.36	0.35	0.060	0.096	0.80	4.87	−3.60	−0.33	3.33	0.98	2.81	2.87
	±0.48	±0.43	±0.016	±0.017	±0.13	±0.22	±0.26	±0.16	±0.43	±0.16	±0.25	±0.37
393-330	−0.03	0.69	0.000	0.024	0.72	3.86	−2.55	−0.23	2.99	0.49	1.76	1.02
	±0.60	±0.55	±0.019	±0.020	±0.23	±0.40	±0.43	±0.27	±0.65	±0.30	±0.45	±0.67
398-341	−1.34	−0.04	0.080	0.108	0.96	5.39	−5.19	−1.04	3.76	0.75	3.11	2.83
	±0.63	±0.58	±0.019	±0.021	±0.23	±0.39	±0.46	±0.29	±0.64	±0.30	±0.43	±0.65
401-344	4.51	3.55	−0.090	−0.054	0.01	1.49	2.69	2.75	0.21	−0.01	0.40	−0.26
	±0.49	±0.44	±0.017	±0.018	±0.17	±0.31	±0.29	±0.18	±0.53	±0.23	±0.35	±0.53
NB 16.....	3.52	2.77	−0.070	−0.035	0.50	2.71	1.30	2.38	1.45	0.37	1.66	1.22
	±0.43	±0.37	±0.015	±0.015	±0.07	±0.14	±0.16	±0.09	±0.35	±0.10	±0.17	±0.25
NB 67.....	3.29	2.71	−0.070	−0.033	0.48	2.73	1.20	2.26	1.44	0.29	1.76	1.09
	±0.45	±0.39	±0.015	±0.016	±0.11	±0.20	±0.21	±0.12	±0.41	±0.15	±0.23	±0.34
NB 68.....	−0.15	0.94	−0.040	−0.017	0.94	5.23	−3.69	−0.43	3.50	0.65	2.50	2.45
	±0.45	±0.39	±0.015	±0.016	±0.10	±0.18	±0.21	±0.13	±0.38	±0.13	±0.21	±0.30
NB 74.....	−2.90	−0.58	−0.020	0.001	1.53	6.44	−6.92	−2.24	5.29	0.67	2.47	2.12
	±0.84	±0.78	±0.024	±0.027	±0.33	±0.58	±0.73	±0.46	±0.90	±0.45	±0.66	±1.00
NB 81.....	0.58	1.20	−0.040	−0.016	0.75	5.25	−3.15	0.15	3.79	0.95	2.76	3.85
	±0.46	±0.41	±0.015	±0.016	±0.12	±0.20	±0.24	±0.15	±0.41	±0.15	±0.24	±0.35

TABLE 4A—*Continued*

Name	$H\delta_A$ (Å)	$H\delta_F$ (Å)	CN_1 (mag)	CN_2 (mag)	Ca4227 (Å)	G4300 (Å)	$H\gamma_A$ (Å)	$H\gamma_F$ (Å)	Fe4384 (Å)	Ca4455 (Å)	Fe4531 (Å)	$C_2$4668 (Å)
NB 83.....	2.61	2.27	−0.060	−0.023	0.66	3.56	0.22	1.96	1.97	0.49	2.09	1.62
	±0.46	±0.41	±0.015	±0.016	±0.12	±0.22	±0.24	±0.14	±0.43	±0.17	±0.26	±0.38
NB 87.....	−3.72	−0.56	0.010	0.048	1.76	5.96	−7.38	−2.19	6.22	1.21	3.24	4.52
	±0.50	±0.43	±0.016	±0.017	±0.12	±0.22	±0.28	±0.17	±0.42	±0.16	±0.25	±0.36
NB 89.....	0.70	1.31	0.050	0.094	0.69	4.04	−1.61	0.84	2.85	0.88	2.65	2.11
	±0.50	±0.44	±0.016	±0.017	±0.13	±0.22	±0.23	±0.14	±0.41	±0.14	±0.22	±0.30
NB 91.....	−0.38	0.84	−0.040	−0.016	0.95	5.25	−3.76	−0.53	3.59	0.70	2.43	2.42
	±0.47	±0.41	±0.015	±0.016	±0.11	±0.20	±0.23	±0.15	±0.40	±0.14	±0.23	±0.33

field and Virgo Cluster and a further 34 galaxies from the central regions of the Coma Cluster. These galaxies cover an absolute magnitude range $-22.5 < M_B < -16.5$ and consist of dwarf to giant elliptical galaxies. All the observations were performed with an $R_e/4$ aperture and are fully corrected to the Lick system. We have "de-corrected" these data (using the offsets kindly supplied by P. Sánchez-Blázquez) in order to directly compare with our data.

Interestingly, there appear to be obvious differences between the loci of the field and Coma Cluster galaxies with respect to the GC data. The field galaxies generally appear to have lower Balmer line strengths when compared to the cluster galaxies at a given [MgFe]. Moreover, there is a suggestion that the locus of the GC data more closely follows that of the field galaxies than of those in clusters. A straightforward (but nonunique) interpretation is that the GCs and field elliptical galaxies are generally older than cluster galaxies. We note that the metallicities (as given by [MgFe]) of the most metal-rich M31 and Galactic GCs do not quite form a continuous relation with the galaxies. However, as noted by P02, the metallicities of the most metal-rich Galactic GCs are comparable to the integrated Milky Way bulge light. This is consistent with the idea that more metal-rich galaxies harbor more metal-rich GC systems (van den Bergh 1975; Brodie & Huchra 1991; Strader et al. 2004).

We see no difference in the Balmer lines of the metal-rich Galactic and M31 GCs at a given value of [MgFe], whereas previous studies (Burstein et al. 1984; Brodie & Huchra 1991) have documented possible differences (at a given value of Mg_2). What is the origin of this disagreement between studies? One possible answer is the S/N; these present data represent an improvement in S/N over the older studies. For example, the mean uncertainty in our $H\beta$ measurements are 0.17 Å, whereas in Burstein et al. (1984) it is 0.26 Å. However, the effect of larger errors in, e.g., $H\beta$ should in principle act to wash out any systematic differences rather than enhance them. As shown in Table 3, the agreement between the P02 and CBR98 data for the indices in question is excellent (with the possible exception of $H\gamma_A$; however, in this case there is only one common cluster between these data sets). For example, the mean difference in the $H\beta$ index for the four clusters in common is only (P02 minus CBR98) -0.0027, $\sigma = 0.13$ Å.

Indeed, in comparison with the CBR98 and P02 data, the $H\beta$ indices from Trager et al. (1998) for their Galactic GC data look systematically low. This is also evident when these data are compared to stellar population models (Beasley et al. 2000; Kuntschner et al. 2002). For the three clusters in common between the P02 data and Trager et al. (1998), the difference is (P02 minus Trager) 0.44 ± 0.28 Å. By comparison, the mean difference in $H\beta$ between the M31 and Galactic clusters with $[\mathrm{MgFe}] > 1.5$ in Trager et al. (1998) is $\sim$0.6 Å, which led Burstein et al. (1984) to conclude that the M31 GCs may exhibit $H\beta$ enhancement.

It is hard to see how these differences have arisen, since the $H\beta$ index is only weakly affected by continuum slope changes or resolution differences. Experiments involving adding synthetic noise to our spectra showed no signs of deviations from Gaussian errors. One possibility is foreground contamination from disk and/or halo stars; however, this is not expected to be a significant effect (P02) and is unlikely to occur for all the metal-rich objects in question. Other possibilities include uncertain sky subtraction, especially in areas of high background (CBR98; P02) and variations in the sampled luminosity of the clusters (P02). On the basis of their thorough analysis of these issues, we prefer the P02 indices over previous measurements.

In any event, on the basis of these present data, we conclude that there is no Balmer line enhancement in this sample of M31 GCs when compared to their Galactic counterparts at high metallicity ($[\mathrm{Fe/H}] \geq -0.8$). At low metallicity, there is some evidence for stronger $H\beta$ and $H\gamma$ in the M31 clusters, which is perfectly consistent with horizontal-branch variations.

4.2. C *and* N *in Globular Clusters*

One of the principal results of the Burstein et al. (1984) study was the identification of strong CN molecular bands (λ4150) in the spectra of M31 clusters. They found that at a given Mg_2 index strength, the CN feature in the M31 clusters was up to 0.1 mag stronger than that seen in elliptical galaxies. However, no convincing comparison could be made with the Galactic GCs because of the lack of the most metal-rich objects in their sample. A similar result was found by Brodie & Huchra (1991) using a similar definition of the near-UV cyanogen feature.

The lack of any significant variation in the G-band (CH) feature was indicative in both studies that C was not the main culprit in the CN enhancement. Subsequent data with the inclusion of the bluer NH feature at λ3360, (Tripicco 1989; Ponder et al. 1998; Li & Burstein 2003) strongly suggests the presence of enhanced N in the integrated spectra of M31 clusters compared with Galactic dwarfs of comparable spectral type.

However, the Galactic GC samples of Burstein et al. (1984) and Brodie & Huchra (1991) did not include the most metal-rich Galactic GCs in which one can expect to see the strongest CN enhancements. Fortunately the P02 data provide such a sample of clusters, and indeed these authors have noted that the CN strengths of the most metal-rich Galactic GCs are significantly enhanced when compared to the integrated spectrum of the (outer) Galactic bulge. Moreover, these authors

TABLE 4B

LICK/IDS INDICES AND UNCERTAINTIES FOR M31 GLOBULAR CLUSTERS: 4800–6000 Å

Name	Hβ (Å)	Fe5015 (Å)	Mg_1 (mag)	Mg_2 (mag)	Mg *b* (Å)	Fe5270 (Å)	Fe5335 (Å)	Fe5406 (Å)	Fe5709 (Å)	Fe5782 (Å)	Na D (Å)	TiO_1 (mag)
126-184	3.63	2.29	0.014	0.066	1.28	1.02	0.81	0.47	0.27	0.16	1.15	0.010
	±0.14	±0.37	±0.015	±0.014	±0.24	±0.17	±0.20	±0.14	±0.11	±0.11	±0.52	±0.010
134-190	1.76	2.85	0.050	0.129	2.22	1.79	1.59	0.99	0.61	0.41	1.75	0.022
	±0.16	±0.38	±0.015	±0.014	±0.24	±0.17	±0.20	±0.15	±0.11	±0.11	±0.52	±0.010
158-213	1.72	3.23	0.074	0.150	2.27	1.86	1.70	1.06	0.62	0.47	2.48	0.020
	±0.10	±0.27	±0.015	±0.013	±0.21	±0.10	±0.13	±0.09	±0.07	±0.07	±0.51	±0.010
163-217	1.72	4.79	0.098	0.242	4.01	2.60	2.44	1.57	0.83	0.76	4.30	0.038
	±0.07	±0.22	±0.015	±0.013	±0.19	±0.07	±0.09	±0.06	±0.04	±0.05	±0.50	±0.010
222-277	4.44	4.10	0.050	0.121	1.30	1.87	1.17	0.97	0.61	0.37	3.25	0.029
	±0.31	±0.72	±0.016	±0.015	±0.39	±0.37	±0.43	±0.31	±0.24	±0.24	±0.58	±0.012
225-280	1.81	4.25	0.089	0.207	3.21	2.31	2.03	1.31	0.79	0.65	3.10	0.027
	±0.07	±0.23	±0.015	±0.013	±0.19	±0.07	±0.09	±0.06	±0.05	±0.05	±0.50	±0.010
234-290	1.70	3.14	0.055	0.133	2.37	2.03	1.50	0.99	0.51	0.46	2.15	0.020
	±0.16	±0.38	±0.015	±0.014	±0.24	±0.18	±0.21	±0.15	±0.12	±0.11	±0.52	±0.010
292-010	3.12	1.67	0.038	0.073	0.97	0.95	1.14	0.15	0.33	0.19	1.32	0.006
	±0.32	±0.76	±0.016	±0.016	±0.40	±0.39	±0.45	±0.34	±0.26	±0.25	±0.60	±0.013
301-022	2.92	2.26	0.022	0.076	1.70	1.43	1.18	0.33	0.56	0.36	1.44	0.008
	±0.33	±0.74	±0.016	±0.015	±0.38	±0.37	±0.42	±0.31	±0.24	±0.23	±0.58	±0.012
304-028	2.50	0.59	0.041	0.070	1.23	1.40	0.92	0.85	0.39	0.26	1.72	0.011
	±0.30	±0.72	±0.016	±0.015	±0.37	±0.36	±0.42	±0.30	±0.24	±0.23	±0.58	±0.012
310-032	2.54	1.45	0.035	0.055	0.92	1.26	0.84	0.44	0.25	0.02	1.57	0.017
	±0.30	±0.70	±0.016	±0.015	±0.36	±0.35	±0.40	±0.29	±0.23	±0.22	±0.57	±0.012
313-036	1.49	3.00	0.060	0.140	2.17	1.69	1.45	0.97	0.66	0.61	2.80	0.024
	±0.21	±0.48	±0.015	±0.014	±0.28	±0.23	±0.26	±0.19	±0.15	±0.14	±0.53	±0.011
314-037	4.70	1.70	0.055	0.122	2.85	1.56	1.89	0.82	0.80	0.31	2.73	−0.004
	±0.52	±1.28	±0.020	±0.020	±0.61	±0.69	±0.79	±0.59	±0.47	±0.47	±0.77	±0.017
321-046	6.83	0.97	0.028	0.052	0.94	0.80	0.73	0.20	0.45	0.35	1.37	0.007
	±0.32	±0.85	±0.017	±0.016	±0.43	±0.45	±0.52	±0.38	±0.30	±0.29	±0.62	±0.013
322-049	5.04	1.23	0.038	0.048	0.35	0.63	0.67	0.45	0.46	0.28	1.68	0.014
	±0.24	±0.62	±0.016	±0.015	±0.34	±0.33	±0.38	±0.28	±0.23	±0.22	±0.58	±0.012
324-051	4.67	3.24	0.045	0.085	1.57	1.66	1.46	0.71	0.55	0.31	0.71	0.019
	±0.14	±0.38	±0.015	±0.014	±0.24	±0.19	±0.22	±0.16	±0.13	±0.13	±0.53	±0.011
327-053	3.76	1.78	0.050	0.077	0.59	0.83	1.10	0.72	0.42	0.60	2.67	0.028
	±0.14	±0.38	±0.015	±0.014	±0.25	±0.19	±0.22	±0.16	±0.13	±0.12	±0.52	±0.011
328-054	2.56	0.78	0.033	0.068	0.19	0.89	0.49	0.40	0.04	0.44	1.88	0.002
	±0.35	±0.81	±0.017	±0.016	±0.42	±0.41	±0.48	±0.35	±0.27	±0.25	±0.59	±0.013
337-068	3.21	2.65	0.013	0.084	1.86	1.48	1.11	0.64	0.44	0.26	1.21	0.006
	±0.07	±0.22	±0.015	±0.013	±0.19	±0.07	±0.09	±0.06	±0.05	±0.05	±0.50	±0.010
347-154	2.85	1.01	0.020	0.044	0.76	0.51	0.49	0.37	0.12	0.11	1.15	0.002
	±0.17	±0.43	±0.015	±0.014	±0.26	±0.21	±0.24	±0.17	±0.14	±0.13	±0.53	±0.011
350-162	2.78	1.59	0.034	0.075	1.13	0.98	0.81	0.33	0.39	0.19	1.00	0.006
	±0.27	±0.63	±0.016	±0.015	±0.34	±0.32	±0.37	±0.27	±0.21	±0.20	±0.56	±0.012
365-284	2.70	2.05	0.040	0.080	1.37	1.33	1.00	0.50	0.43	0.31	2.54	0.014
	±0.17	±0.43	±0.015	±0.014	±0.26	±0.20	±0.24	±0.18	±0.14	±0.13	±0.53	±0.011
380-313	6.05	2.74	0.038	0.080	1.19	1.86	1.36	0.64	0.50	0.42	1.96	0.026
	±0.22	±0.57	±0.016	±0.014	±0.32	±0.29	±0.34	±0.26	±0.21	±0.20	±0.56	±0.012
383-318	1.73	3.95	0.070	0.183	3.03	2.12	1.79	1.21	0.63	0.51	2.38	0.028
	±0.13	±0.33	±0.015	±0.013	±0.22	±0.14	±0.17	±0.12	±0.09	±0.09	±0.51	±0.010
393-330	1.88	2.82	0.069	0.122	1.49	1.93	1.58	0.70	0.59	0.48	1.92	0.018
	±0.24	±0.57	±0.016	±0.014	±0.32	±0.28	±0.33	±0.24	±0.19	±0.18	±0.55	±0.011
398-341	1.58	3.86	0.086	0.182	3.17	2.31	1.71	1.07	0.65	0.45	2.49	0.028
	±0.24	±0.55	±0.016	±0.014	±0.30	±0.27	±0.31	±0.23	±0.18	±0.17	±0.54	±0.011
401-344	2.82	0.59	0.034	0.047	0.53	0.63	0.53	−0.03	−0.01	0.06	0.93	0.005
	±0.19	±0.47	±0.015	±0.014	±0.27	±0.23	±0.27	±0.20	±0.16	±0.15	±0.54	±0.011
NB 16.....	3.32	2.31	0.023	0.086	1.61	1.18	0.97	0.50	0.39	0.20	1.16	0.006
	±0.08	±0.25	±0.015	±0.013	±0.20	±0.09	±0.11	±0.08	±0.06	±0.07	±0.51	±0.010
NB 67.....	3.29	2.38	0.023	0.081	1.65	1.12	0.79	0.47	0.32	0.23	1.14	0.003
	±0.12	±0.32	±0.015	±0.013	±0.22	±0.14	±0.17	±0.12	±0.09	±0.09	±0.51	±0.010
NB 68.....	2.30	3.09	0.033	0.145	3.22	1.98	1.59	0.90	0.59	0.40	1.51	0.005
	±0.10	±0.28	±0.015	±0.013	±0.21	±0.12	±0.14	±0.10	±0.08	±0.08	±0.51	±0.010
NB 74.....	1.22	2.95	0.080	0.239	5.17	1.82	1.83	0.97	0.72	0.34	3.10	−0.003
	±0.38	±0.86	±0.017	±0.016	±0.42	±0.45	±0.52	±0.39	±0.31	±0.30	±0.62	±0.013
NB 81.....	2.83	4.05	0.041	0.142	2.72	2.19	1.75	0.90	0.78	0.48	1.51	0.002
	±0.12	±0.33	±0.015	±0.013	±0.22	±0.14	±0.17	±0.12	±0.10	±0.10	±0.51	±0.010

TABLE 4B—*Continued*

Name	Hβ (Å)	Fe5015 (Å)	Mg_1 (mag)	Mg_2 (mag)	Mg *b* (Å)	Fe5270 (Å)	Fe5335 (Å)	Fe5406 (Å)	Fe5709 (Å)	Fe5782 (Å)	Na D (Å)	TiO_1 (mag)
NB 83	3.21	2.63	0.023	0.087	1.79	1.44	1.09	0.42	0.38	0.26	1.18	0.004
	±0.13	±0.35	±0.015	±0.014	±0.23	±0.16	±0.19	±0.14	±0.11	±0.11	±0.52	±0.010
NB 87	1.59	4.29	0.089	0.277	5.19	3.25	2.85	1.88	0.98	0.75	2.99	0.006
	±0.13	±0.33	±0.015	±0.013	±0.22	±0.14	±0.17	±0.12	±0.09	±0.09	±0.51	±0.010
NB 89	2.02	3.28	0.054	0.143	2.43	1.91	1.63	1.02	0.59	0.50	3.08	0.019
	±0.09	±0.26	±0.015	±0.013	±0.20	±0.09	±0.11	±0.07	±0.06	±0.06	±0.50	±0.010
NB 91	2.17	3.32	0.034	0.145	3.19	1.96	1.76	0.98	0.65	0.37	1.79	0.004
	±0.12	±0.30	±0.015	±0.013	±0.21	±0.13	±0.16	±0.11	±0.09	±0.09	±0.51	±0.010

also commented that these most metal-rich Galactic GCs in their sample have similar CN strengths to the M31 sample of Trager et al. (1998).

In Figure 3 we show the Lick CN_2 index for the M31 and Galactic GC data at a given [MgFe]. We show the CN_2 index rather than CN_1, since this latter index suffers from contamination from the adjacent Hδ feature. Note that the CBR98 data generally do not reach down to ∼4000 Å, and therefore we rely on the P02 data set for comparison to these M31 data. Figure 3 suggests that the CN indices for the Galactic and M31 clusters are all significantly enhanced with respect to the bulges of the Milky Way and M31. This is consistent with the findings of Burstein et al. (1984) and P02. The difference in CN_2 between the Milky Way outer bulge observations and the M31 and P02 data at the same value of [MgFe] is ∼0.07 mag.

We have also plotted CN_2 data from the field and cluster sample of elliptical galaxies from Sánchez-Blázquez et al. (2003). As discussed by these authors, the CN_2 indices of the field and Coma Cluster elliptical galaxies appear to show different behavior; field elliptical galaxies appear more enhanced in CN than those in the denser environment of Coma. Indeed, the locus of the field galaxies is closer to that of the GCs, although there still appears to be a substantial offset between the two. Sánchez-Blázquez et al. (2003) concluded that both N and C were enhanced in the field relative to cluster elliptical galaxies, possibly through pollution of the ISM through low- and intermediate-mass stars.

We see no strong evidence for an enhancement in CN_2 in the M31 clusters with respect to the Galactic GCs at any metallicity. Similar behavior is seen in the CN_1 index. This is a rather

TABLE 5
LINEAR FIT COEFFICIENTS: CBR98 GALACTIC CLUSTER DATA

Index	*a*	*b*	rms	Lick minus CBR98	σ_{rms}	*N*
$H\delta_A$	...	...	...	...	...	...
$H\delta_F$	0.6108	−1.3760	...	0.2210	1.1430	2[a]
CN_1	0.0725	−1.0540	...	0.0210	0.0537	2[a]
CN_2	0.0052	0.8462	...	0.0020	0.0057	2[a]
Ca4227	0.2373	0.4451	0.0631	0.1067	0.3919	4[b]
G4300	0.2390	1.0550	0.4266	−0.4015	0.5039	4[b]
$H\gamma_A$	−1.1790	2.4030	0.1657	0.5383	2.3030	3
$H\gamma_F$	−0.1537	0.9790	0.7687	0.1710	0.8882	4
Fe4383	0.4878	0.5728	0.3304	0.6123	1.0930	4[b]
Ca4455	−0.1364	0.5420	0.0373	0.5220	0.2441	5
Fe4531	−0.3698	1.0900	0.0702	0.1987	0.1172	4[b]
$C_2$4668	0.2719	0.7662	0.4248	0.0274	0.5502	5[b]
Hβ	0.2606	0.8592	0.1256	0.0077	0.1570	6
Fe5015	−0.3993	1.0290	0.2905	0.3152	0.3202	6
Mg_1	0.0002	1.1940	0.0171	−0.0068	0.0192	6
Mg_2	0.0091	0.9802	0.0010	−0.0070	0.0017	6
Mg *b*	−0.0859	1.0300	0.1239	0.0275	0.1392	6
Fe5270	0.0543	0.9417	0.2217	0.0348	0.2461	6
Fe5335	0.3537	0.8841	0.2172	−0.2305	0.2492	6
Fe5406	−0.1683	1.0310	0.0463	0.1390	0.0526	6
Fe5709	0.1194	0.7490	0.1511	0.0106	0.1934	5[b]
Fe5782	0.0567	0.8221	0.1144	0.0180	0.1345	6
Na D	0.1374	0.8028	0.1840	0.2898	0.2990	6
TiO_1	0.0078	0.5477	0.0068	0.0005	0.0112	6
TiO_2	−0.0102	1.3910	0.0154	−0.0052	0.0199	4

NOTES.—Linear fit coefficients, rms of linear fit, mean difference, and its standard deviation between the CBR98 Galactic cluster data and Trager et al. (1998) Galactic clusters. Lick indices for Hδ and Hγ are taken from Kuntschner et al. (2002). The value *N* signifies the number of clusters with common indices. Indices measured using the Trager et al. (1998) and Worthey & Ottaviani (1997) Lick index definitions.

[a] No rms calculated for $N < 3$.

[b] Index measurement for NGC 6171 excluded from fit.

TABLE 6
Linear Fit Coefficients: LRIS M31 Globular Cluster Data

Index	a	b	rms	Lick minus M31	$\sigma_{\rm rms}$	N
Hδ_A	−1.5190	−0.4680	...	−1.2330	1.0690	2[a]
Hδ_F	0.6042	0.2634	0.0143	−0.0370	0.7143	3
CN_1	0.0308	1.0480	0.0048	−0.0337	0.0065	3
CN_2	0.0334	0.9869	0.0063	−0.0320	0.0078	3
Ca4227	0.4951	0.4415	0.1514	−0.0967	0.2211	3
G4300	−0.1284	1.0120	0.1967	0.0733	0.2410	3
Hγ_A	5.3500	1.9070	...	−0.6725	0.5197	2[a]
Hγ_F	−0.2218	0.6410	0.1045	0.1500	0.3576	3
Fe4383	4.5760	−0.2190	0.6566	0.0233	0.9420	3
Ca4455	−0.3685	1.0790	0.0962	0.2720	0.1196	3
Fe4531	1.0450	0.6931	0.0273	−0.2370	0.2176	3
$C_2$4668	1.8400	0.4738	0.2666	−0.5613	1.1520	3
Hβ	1.4620	0.1640	0.0273	0.0150	0.2247	3
Fe5015	0.9523	0.7859	0.2682	−0.0973	0.3823	3
Mg_1	0.0646	0.4040	0.0066	−0.0317	0.0156	3
Mg_2	0.0236	0.9728	0.0031	−0.0187	0.0040	3
Mg b	−0.5430	1.2040	0.0946	−0.0840	0.1863	3
Fe5270	−0.0404	0.9489	0.1330	0.1640	0.1639	3
Fe5335	0.4890	0.8229	0.1629	−0.1513	0.2104	3
Fe5406	−0.5510	1.6110	0.1155	−0.1560	0.1633	3
Fe5709	0.4219	0.3616	0.0688	0.1527	0.1622	3
Fe5782	0.4351	0.2569	0.0846	0.1173	0.3092	3
Na D	−0.5590	1.1620	0.1179	0.0210	0.1932	3
TiO_1	0.0186	0.4208	0.0032	−0.0053	0.0119	3
TiO_2	...	...	...	...	...	...

Notes.—Linear fit coefficients, rms of linear fit, mean difference, and its standard deviation between the three clusters in common between the LRIS M31 globular cluster data and Trager et al. (1998). Lick indices for Hδ and Hγ are taken from Kuntschner et al. (2002). Lick index definitions are given in Trager et al. (1998) and Worthey & Ottaviani (1997).

[a] No rms calculated for $N < 3$.

surprising result, considering the fact that the CN enhancement in M31 clusters has been well documented (Burstein et al. 1984; Tripicco 1989; Davidge 1990; Tripicco & Bell 1990; Brodie & Huchra 1991; Ponder et al. 1998; Li & Burstein 2003). Our findings do not appear to be an artifact of not correcting to the Lick system, which actually exacerbates the problem, since the correction is significant (0.032 mag for CN_2). Through experimentation, we find that both CN_1 and CN_2 can vary by up to several tenths of a magnitude depending upon the details of our flux calibrations, but this is generally only true for the very metal-poor clusters, which have relatively large amounts of blue flux. This problem is particularly acute in the blue part of the spectrum for broad indices, since the throughput of the "pre–blue-arm" LRIS rolls off rapidly at ∼4000 Å.

We have, however, measured the near-UV cyanogen index at λ3883 (using the definitions given in Brodie & Huchra 1990) for the M31 and P02 data, which through experimentation appears to be much less sensitive to our flux calibration uncertainties.[8] The CN index at λ3883 is also significantly stronger than the Lick CN indices.

The strength of the blue cyanogen index (CNB) with [MgFe] is plotted in Figure 4. The difference in CNB between the M31 and Galactic GCs is startling and is evident at all metallicities. The metallicity range in which we can perform a direct comparison between the M31 and Galactic GCs is defined by the P02 data, with $-1.48 \leq [\mathrm{Fe/H}] \leq -0.34$. At $[\mathrm{Fe/H}] \sim -1.5$, the mean difference between the Galactic and M31 data is $\Delta\mathrm{CNB} \sim 0.1$ mag. For the most metal-rich GCs at $[\mathrm{Fe/H}] \sim -0.4$, $\Delta\mathrm{CNB} \sim 0.2$ mag.

To check the reality of this result, since Lick CN_2 and CNB appear to disagree, we have taken one of the "CN-weak" Galactic GCs, NGC 6441, the spectrum of which was kindly supplied by T. Puzia, and divided it by one of the "CN-strong" M31 clusters (225-280). These clusters have very similar [MgFe] strengths (i.e., very similar metallicities), and care was taken to ensure these spectra were at the same normalization, resolution, and spectral sampling. This residual spectrum is shown in Figure 5.

CNB in the residual spectrum is clearly enhanced, indicating that the M31 GC has significantly stronger CN absorption than NGC 6441 at the same metallicity. Weak enhancement is also seen in the Lick CN index, an enhancement that is washed out at lower metallicities. G4300 also appears to be mildly enhanced. Since this index measures CH, this would suggest that C is also mildly enhanced (see below).

On the basis of the clear differences in the CNB index that we observe, we conclude that CN is enhanced in the M31 GCs with respect to their Galactic counterparts at all metallicities. The lack of obvious enhancement in the CN_1 and CN_2 indices between the Galactic and M31 clusters probably reflects the relatively low sensitivities of these indices to CN when compared to CNB rather than any systematic offset between these data (see Trager 2004 for a discussion of this issue).

Variations in CN are thought to be controlled largely by variations in N, since free C is rapidly incorporated into the CO molecule. Therefore, CN "enhancement" is believed to

[8] The truth of this statement is both data-dependent and index-definition–dependent. For example, the single-sided 3883 Å index often used in stellar studies is prone to significant zero-point offsets (e.g., Cohen et al. 2002).

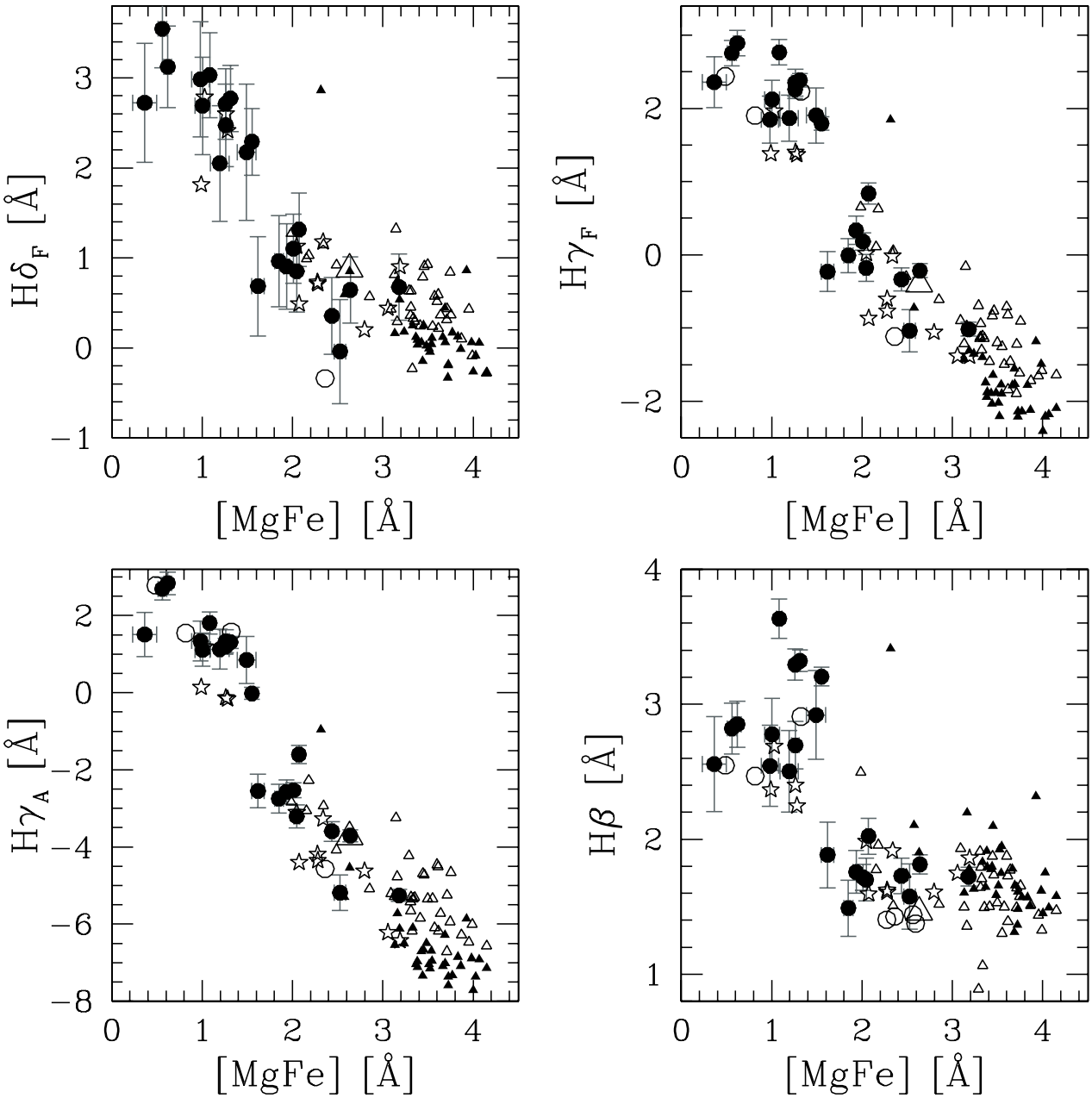

FIG. 2.—Comparison between the M31 data (*filled circles*) and Galactic GC data (*open circles*, CBR98; *stars*, P02) for the Hβ, Hγ, and Hδ Lick indices at a given [MgFe]. Uncertainties (*error bars*) are only shown for M31 data for the sake of clarity. The large open triangles indicate the outer Galactic bulge observations of P02. Small open and filled triangles represent data for Coma and field elliptical galaxies (Sánchez-Blázquez et al. 2003), respectively. For the metal-rich M31 GCs, we see no significant enhancement in the Balmer lines compared to the Galactic data.

reflect an enhancement in N, and this picture is supported through observations of the NH molecule (Ponder et al. 1998; Li & Burstein 2003). However, can we rule out carbon variations? Two Lick indices primarily sensitive to C are the C_2 Swan band $C_2$4668 (formerly Fe4668) and G4300, which measures CH.

In Figure 6 we plot $C_2$4668 as a function of [MgFe]. These data define a very tight sequence in this plot, with a clear change of slope at [MgFe] ~ 3, showing the transition from GCs to galaxies. On the basis of Figure 6, we see no evidence for differences in C among the GCs. However, as discussed by Sánchez-Blázquez et al. (2003), this index is enhanced in field elliptical galaxies with respect to cluster elliptical galaxies at a given metallicity. The behavior of the other carbon-sensitive index, G4300, is plotted in Figure 7. In this case, there is a suggestion that at [MgFe] > 2, the M31 GCs do have stronger G4300 indices than the Galactic GCs. The M31 clusters also have significantly stronger G4300 indices than the outer bulge observations of the Milky Way. Unfortunately, the interpretation of such variations in G4300 are complicated by the fact that this index is also sensitive to age and the O and Ti abundances.

5. YOUNG STAR CLUSTERS IN M31

Eight of the initial 42 GC candidates in the M31 sample exhibit mid-A to early F-type spectra, as would be expected of A–F stars or young star clusters. The existence of very young clusters in the M31 system has been mentioned previously by Huchra et al. (1991) and Barmby et al. (2000).

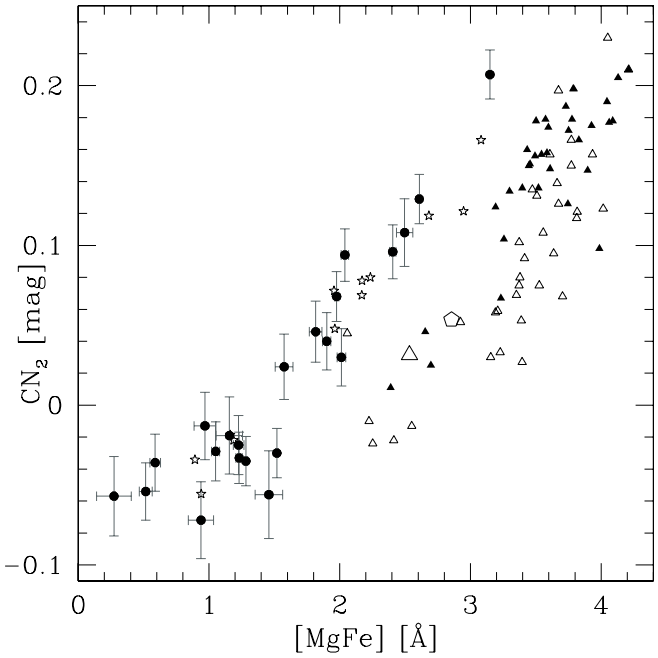

FIG. 3.—Lick CN_2 index as a function of [MgFe] for the M31 GCs (*circles with error bars*) and P02 Galactic GC data (*stars*). The open triangle represents the mean Galactic bulge measurement from P02, and the pentagon denotes the M31 nuclear measurement of Trager et al. (1998). Small filled and open triangles represent data for field and Coma elliptical galaxies, respectively (Sánchez-Blázquez et al. 2003).

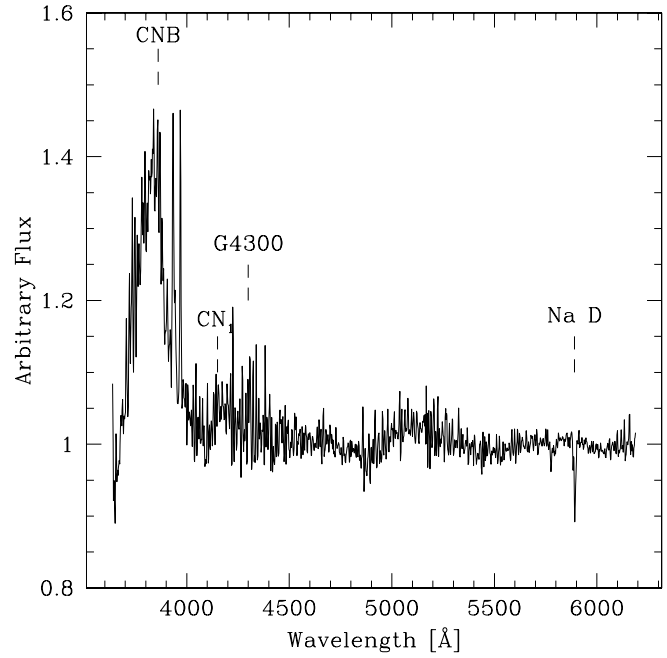

FIG. 5.—Residual spectrum after the spectrum of NGC 6441, a Galactic GC, was divided by that of 225-280, a GC in M31. Both these clusters have [Fe/H] ~ -0.5. The absorption system at CNB is clearly enhanced, indicating greater CN absorption in the M31 GC. The Na D residual probably reflects the contribution of interstellar sodium absorption in the spectrum of the Galactic GC.

One of these clusters, 324-051, is also designated Hubble V in NGC 205 and was taken as a reference template for the other candidate young clusters in M31. Hubble V was identified by Da Costa & Mould (1988) as being a young object from 3 Å resolution optical integrated spectra. On the basis of its similarity to the Small Magellanic Cloud cluster NGC 419, Da Costa & Mould (1988) concluded that Hubble V was $\sim$1 Gyr old but could not rule out ages several gigayears older than this or as young as 100 Myr.

From the broad Balmer lines, weak metal lines, and relatively blue continua of the cluster spectra in our sample, we assign the clusters spectral types A5–F0. Such $\sim$2 $M_\odot$ stars,

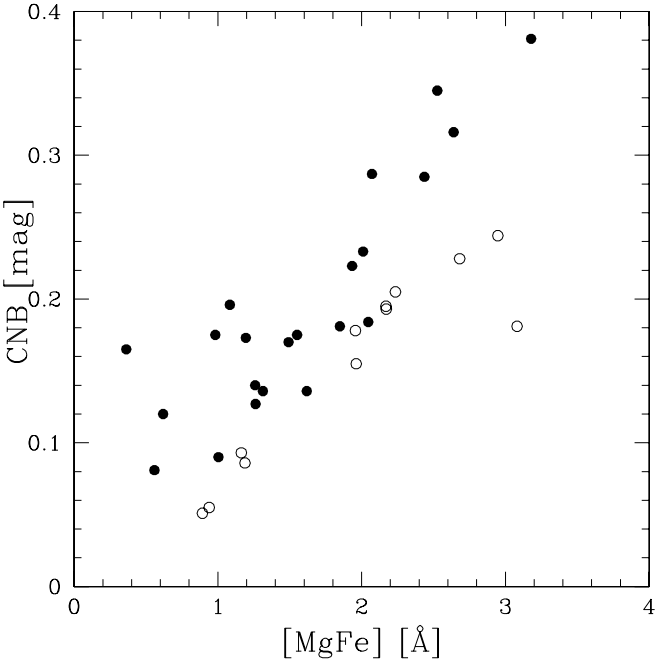

FIG. 4.—Strength of the blue cyanogen index (CNB) at a given [MgFe] for our M31 data (*filled circles*) and the Milky Way GC data of P02 (*open circles*). The M31 GCs appear clearly enhanced with respect to Galactic GCs at all metallicities.

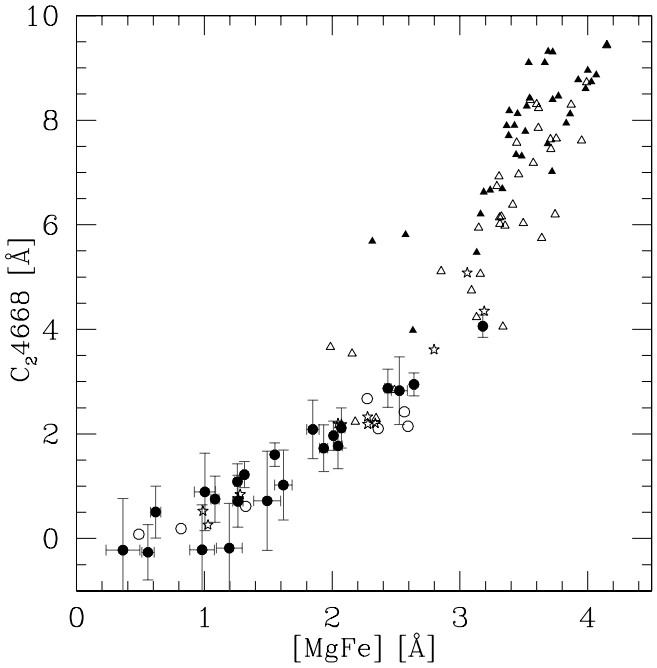

FIG. 6.—Lick $C_2$4668 index as a function of [MgFe]. Symbols are the same as Fig. 3.

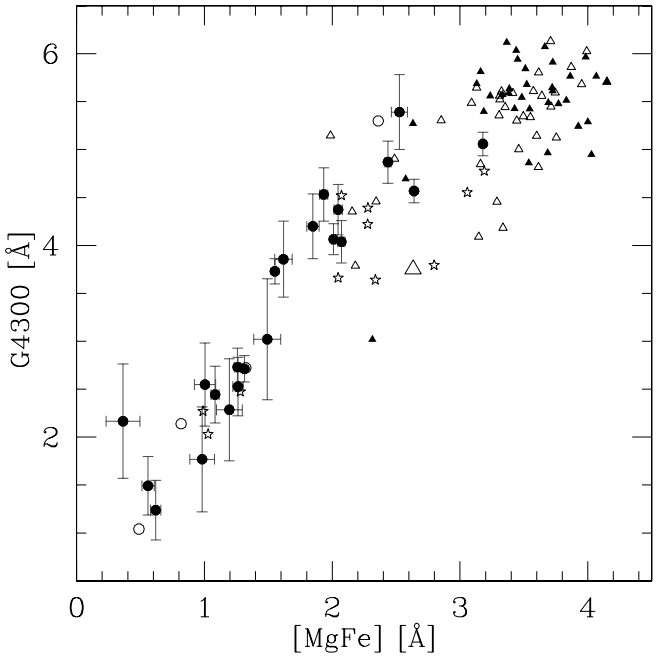

FIG. 7.—Same as Fig. 6, but for the G4300 (CH) index.

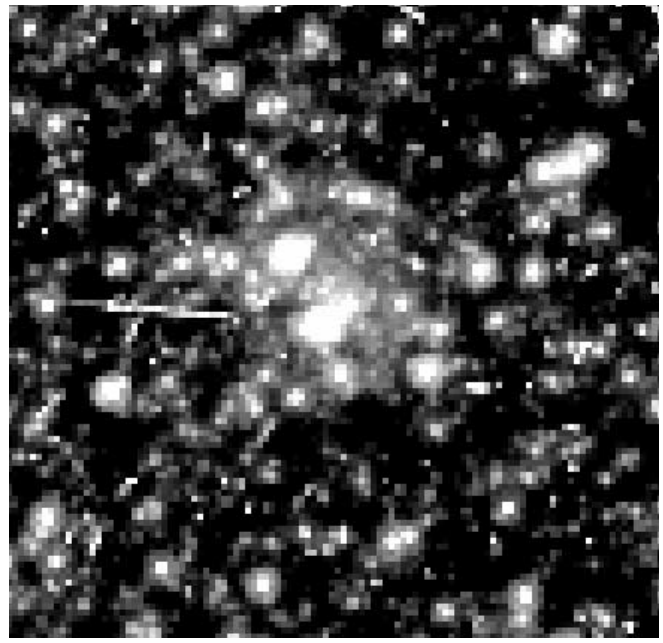

FIG. 9.—*HST*/PC F814W image of the young cluster in NGC 205, Hubble V. The image is 5″ across, which, at the distance of M31, corresponds to a physical diameter of ∼17 pc. The pixel scale of the PC chip is 0.″045 pixel^{-1}.

which dominate the main-sequence turnoff, complete core hydrogen burning after approximately 1 Gyr (Schaller et al. 1992), consistent with the age of Hubble V found by Da Costa & Mould (1988).

The spectra of these cluster candidates are shown in Figure 8. Clear evolution in several indices can be seen as we proceed to later types in the figure; the Balmer lines all weaken, the ratio of Ca II K to Ca II H + Hϵ increases as metal lines strengthen and Hϵ weakens, and the G band (G4300 in the Lick definition), which measures the CH molecule, starts to appear in the Hubble V spectrum and later types. The slope of the spectra also noticeably change from bluer to redder, although reddening also seems to be playing a role here (e.g., 321-046). The cluster 222-227 displays a rather unusual shape, possibly due to heavy reddening, leading to its "peculiar" designation in Table 1. It also happens to be our lowest S/N spectrum.

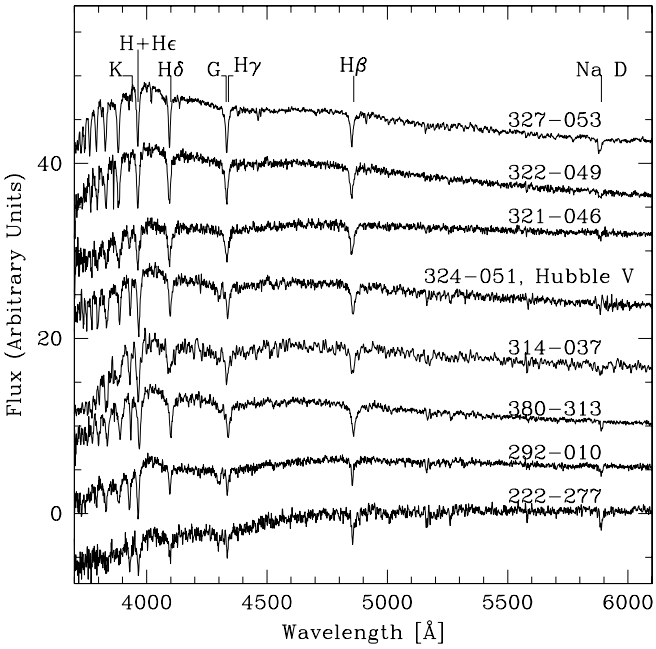

FIG. 8.—LRIS spectra at ∼5.6 Å resolution for the eight candidate young GCs in the M31 sample. The spectra have been normalized, with additive constants on the *y*-axis for display purposes. The spectra are arranged in approximate order of spectral type, running from earlier (A5) to later types (F0; *top to bottom*).

The first obvious question to ask of these young cluster candidates is: are these really globular clusters belonging to M31? In the original Bologna group catalog (Battistini et al. 1987), which was based on photographic plates, all the clusters for which we have spectra are designated A or B classes, i.e., high-confidence clusters, on the basis of their nonstellarity and circularly symmetric brightness distributions. This effectively rules out that these objects are foreground Galactic blue horizontal-branch stars or blue stragglers.

As evidenced by the Large Magellanic Cloud (LMC) system of star clusters, the separation of open and globular clusters is not always clear (e.g., Hodge & Wright 1967). However, the distinction made is usually one of mass and compactness. The absence of high-resolution imaging for all the candidates precludes the secure identification of these objects.[9] However, *Hubble Space Telescope* (*HST*)/WFPC2 imaging does exist for Hubble V (cycle 6, proposal ID 6699, PI D. Geisler). We show the PC chip image of this object in the F814W filter in Figure 9. The cluster is clearly resolved into stars, and Kim et al. (2002) have measured surface brightness profiles for this cluster, finding that it is better fitted by a King (1966) model than a power law, which is usually applicable for open clusters (Elson et al. 1987). Kim et al.'s derived concentration parameter of $c = 0.5$ is comparable to that of the small Milky Way cluster AM-4 (Madore & Arp 1982). The mass-to-light ratios of young clusters evolve

[9] We are currently pursuing such imaging for these objects.

rapidly because of the short main-sequence lifetimes of massive stars; this in turn strongly affects any mass estimates for the clusters. We return to estimating the cluster masses later when we have more secure age determinations for these objects.

Age-dating young stellar populations (<1 Gyr) from integrated spectra presents a different set of challenges from older stellar systems. For stellar populations older than $\sim 2\times 10^8$ yr, Balmer lines decrease monotonically with time and can be used to estimate the age of the system (e.g., Bruzual & Charlot 2003). The key difficulty lies in determining the metallicity of the stellar population, since metal lines become very weak in young objects (e.g., Larsen & Brodie 2002). We have taken two approaches: first we compare the M31 spectra with a series of LMC templates (Beasley et al. 2002b) that bracket the expected age range, and then we use stellar population models to provide independent age and metallicity information on the clusters. The two approaches are complementary and provide useful insight into the reliability of each method.

The LMC cluster system consists of clusters with a range of metallicities and ages, from very metal-poor "classical" globular clusters to intermediate-aged and young, near–solar metallicity star clusters (e.g., Olsen et al. 1998; Geisler et al. 2003; Piatti et al. 2003).[10] This range of cluster types provides an excellent source of templates for more distant studies (Leonardi & Rose 2003). Beasley et al. (2002b) published integrated spectra of 24 LMC star clusters with "SWB types" (Searle et al. 1980, hereafter SWB80) ranging from IVA to VII. While the exact age calibration of the SWB80 system is still a source of uncertainty, using the calibration of Bica et al. (1992), these types correspond to ages of roughly 0.20–16 Gyr. The earlier calibration of Cohen (1982) gives somewhat older ages for the intermediate SWB types (III–VI).

Spectra for SWB I–III clusters (0.01–0.20 Gyr) were also obtained by Beasley et al. (2002b) but remained unpublished, since the stellar population models assessed did not extend to such young ages. We have used the full sample of Beasley et al. (2002b), which consists of 65 clusters, the majority of which are less than 1 Gyr old. In order to obtain the best match between the young M31 clusters and the LMC templates, we cross-correlate each M31 spectrum against the entire LMC library and select the LMC cluster that yields the highest (normalized) cross-correlation peak height. For this purpose, the M31 spectra were smoothed and resampled to match the natural resolution of the LMC data (6.5 Å). The spectra were then normalized by a low-order polynomial (since the LMC data are not flux-calibrated) and cross-correlated in the wavelength interval 4000–5400 Å, which is the effective wavelength range of the LMC data.

To test the method, we first cross-correlated the M31 cluster 324-051 (Hubble V) against the LMC library, since we have some independent age information for this cluster. Da Costa & Mould (1988) determined an age of $\sim$1 Gyr for this cluster, with a lower bound of 100 Myr, whereas Lee (1996) determined from his measured color of the cluster ($B-V_0 = 0.33$) that the cluster is closer to 300 Myr. The best correlation template we obtain for Hubble V is NGC 1940, an SWB II cluster with $B-V \sim 0.3$ (Bica et al. 1992). SWB II corresponds roughly to ages 30–70 Myr, which is surprisingly young.

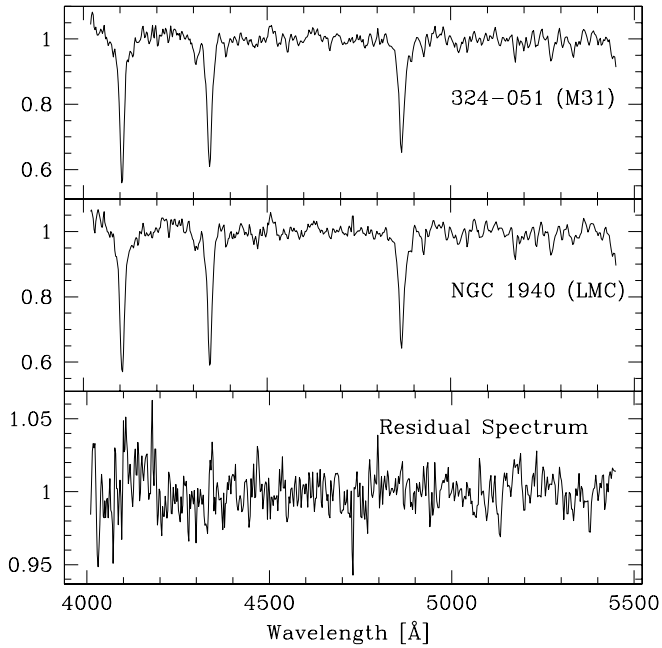

Fig. 10.—Comparison of the normalized spectra of 324-051 (Hubble V; *top*) and NGC 1940 (*middle*), which yielded the highest cross-correlation peak of all the LMC library (Beasley et al. 2002b). The bottom panel shows the residual spectrum after dividing 324-051 by NGC 1940.

The normalized spectra of Hubble V and NGC 1940 are shown in Figure 10. The two clusters look rather similar, and this is supported by examination of the residual spectrum (dividing the Hubble V spectrum by that of NGC 1940). Apart from the mild "P Cygni" profile near Hγ, the residuals are relatively modest. There also appears to be a slight enhancement in the CN residuals, in the sense that CN is lower in Hubble V, although the reality of this is unclear at present.

The next closest templates are NGC 2127 and NGC 2041, which are SWB III and II types, respectively, corresponding to an age range of 30–200 Myr using the Bica et al. (1992) calibration. Girardi et al. (1995) obtained an age of $\sim$100 Myr for NGC 2041 based on a calibration of the photometric *S*-parameter, slightly older than the Bica et al. calibration predicts. The work of Cohen (1982) suggests that SWB III types are closer to 500 Myr. This is an appreciable age range, particularly when one considers that a 30 Myr cluster will be dominated by B stars, whereas in a 500 Myr stellar population A–F stars will be the dominant source of light. The spectrum of Hubble V (Fig. 8) suggests a population of stars cooler than B, closer to late A, due to the presence of metal lines (particularly G-band) in the spectra, and the rollover in the spectrum at $\sim$4000 Å. On the basis of the spectrum alone, the cluster is unlikely to be significantly younger than 100 Myr. Moreover, it should be noted that if the LMC templates are more metal-poor than the M31 clusters (a distinct possibility considering the mass-metallicity relation of galaxies), then because of the age-metallicity degeneracy a younger, more metal-poor LMC template will yield the best correlation match with a slightly older, more metal-rich M31 cluster.

To conclude, we obtain an age determination for Hubble V of 100–500 Myr, in good agreement with previous determinations, under the assumptions that the chemical composition

[10] The age-metallicity relation for the LMC clusters is not continuous. It has been known for some time that there is an "age gap" between 3 and $\sim$10 Gyr (e.g., Jensen et al. 1988) with a corresponding "metallicity gap" at [Fe/H] ~ -1 (Olszewski et al. 1991). This, however, is not a concern for the present study, since we are interested in LMC cluster templates that are younger than a few gigayears.

TABLE 7

Results of Cross-Correlation between Young M31 Clusters and the LMC Templates of Beasley et al. (2002b)

ID	LMC 1	LMC 2	LMC 3	Age range (Gyr)
327-053	SL 106 (I)	NGC 2002 (I)	NGC 1863 (I)	0.01–0.03
322-049	NGC 2031 (III)	NGC 1735 (II)	NGC 1815 (I)	0.01–0.20
380-313	NGC 1735 (II)	NGC 2031 (III)	NGC 1755 (II)	0.01–0.20
321-046	NGC 2031 (III)	NGC 1735 (II)	NGC 1774 (II)	0.01–0.20
324-051	NGC 1940 (II)	NGC 2041 (II)	NGC 2127 (III)	0.01–0.20
314-037	NGC 2127 (III)	NGC 2041 (II)	NGC 1878 (IVA)	0.03–0.40
222-277	NGC 1878 (IVA)	NGC 2127 (III)	NGC 1806 (V)	0.07–2.00
292-010	NGC 1852 (V)	NGC 1751 (V)	NGC 1718 (VI)	0.80–2.0

Notes.—"LMC 1–3" denote the first, second, and third best template matches for the M31 cluster in question. Roman numerals in parentheses denote SWB type, originally defined by SWB80. Age-SWB calibration from Bica et al. (1992).

of the young M31 clusters (metallicity and abundance ratios) are similar to those of the LMC system.

We have performed the previous exercise for the remaining young M31 spectra, each time choosing the three closest cross-correlation templates to the cluster in question. Our results are summarized in Table 7. According to the LMC templates, the M31 clusters span a significant range of ages from 10–30 Myr (327-053) up to 0.8–2 Gyr (292-010). The relative age rankings are qualitatively supported by the appearance of the cluster spectra in Figure 8.

We now appeal to the predictions of stellar population models for more information regarding these objects. To estimate their the ages and metallicities we have employed the evolutionary population synthesis models of Bruzual & Charlot (2003, hereafter BC03). In the optical range in which we are interested (3670–6200 Å), the BC03 models employ the recent stellar library (STELIB) of Le Borgne et al. (2003). The library, which consists of 249 stars taken at a resolution of 3 Å (FWHM), covers with varying degrees of completeness the metallicity range $-2.0 < [\mathrm{Fe/H}] < +0.50$, luminosity classes I–V, and spectral types O5–M9. Perhaps the most serious limitation of these (and other) models for our purposes is the lack of hot stars ($T_{\mathrm{eff}} > 10,000$ K) at nonsolar metallicities. This, however, should not be too problematic, since we expect the abundances of the young M31 clusters to be at or near solar metallicity.

We show in Figure 11 the evolution of the Lick-defined Hβ index as a function of age and metallicity. The models shown adopt the Chabrier (2003) initial mass function (IMF), with a lower mass cutoff of 0.1 $M_{\odot}$ and an upper mass cutoff of 100 $M_{\odot}$. The use of a Salpeter IMF has little effect on the optical indices in question here (BC03). According to the BC03 models, the Hβ index increased rapidly with time until ~300 Myr, when turnoff A stars come to dominate the integrated light. The strength of the index then decreases monotonically with age. In this regime, age is the single most important influence on this index, whereas metallicity is a significant but less important contributor. We have plotted our Hβ measurements for the eight young clusters in Figure 11, which range from 3.12 to 6.83 Å. In themselves, these suggest an age range between 0.02 and 5 Gyr. The higher order Balmer lines show very similar behavior to that of Hβ.

As has been noted before, the relatively narrow definition of the Lick Hβ index is not particularly well suited for very young stellar populations (e.g., Larsen & Brodie 2002). However, we do not rely solely on the Balmer lines for age discrimination. Following the method outlined in Proctor et al. (2004), we have determined the ages and metallicities of the clusters by fitting all our measured Lick indices to the predictions of the BC03 models. Using the entire set of Lick indices maximizes the amount of age and metallicity information present in the spectra, since each index is individually sensitive to age and metallicity (and chemical abundance ratio variations; Proctor & Sansom 2002). This approach is particularly useful in this case, since in these young clusters the metal lines are extremely diluted.

BC03 provide Lick indices for their model spectral energy distributions (SEDs), which cover the age range 0.125 Myr–20 Gyr and a metallicity range of 0.0001–0.05 $Z_{\odot}$. In this case, we use Lick indices measured off the BC03 SEDs, not those derived using the Lick fitting functions, since our data are not corrected to the Lick system. As is the case for the Lick stellar library, the STELIB library is based on solar-neighborhood

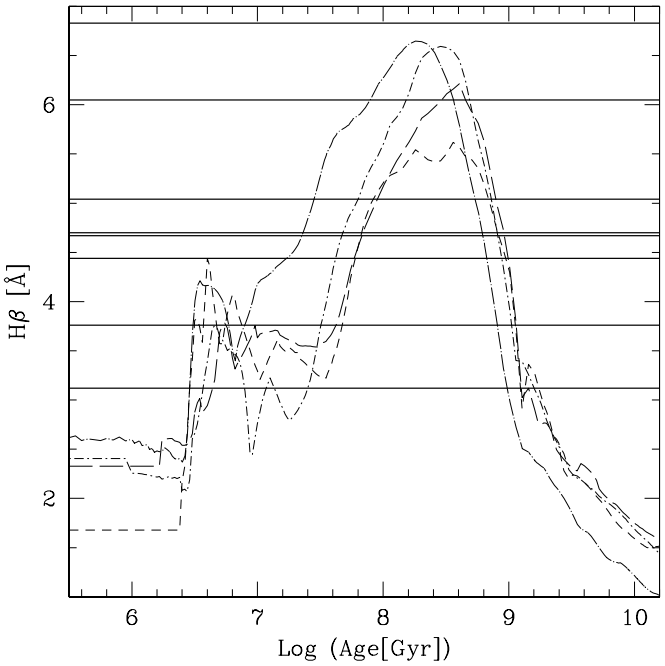

Fig. 11.—Evolution of the Lick Hβ index according to the Bruzual & Charlot (2003) evolutionary population synthesis models, adopting the Chabrier (2003) IMF. Curves in different line types represent metallicities $Z_{\odot}$ ([Fe/H]) 0.004 (−0.64), 0.008 (−0.33), 0.02 (0.09), and 0.05 (0.56) with short-dashed, long-dashed, dot–short-dashed, and dot–long-dashed lines, respectively. The thick horizontal lines are the Hβ measurements of the eight young clusters.

TABLE 8
Best Matches to the BC03 Stellar Population Models

ID	[Fe/H]	Age (Gyr)	N	M/L_V	Mass ($M_\odot$)	Velocity (km s^{-1})
327-053	0.300 ± 0.750	0.080 ± 0.929	18	0.092	2.1×10^4	−542 ± 56
322-049	−0.200 ± 0.200	0.102 ± 0.470	24	0.104	7.0×10^3	−576 ± 21
380-313	0.150 ± 0.100	0.454 ± 0.133	24	0.250	4.1×10^4	−115 ± 24
321-046	0.000 ± 0.600	0.286 ± 0.280	24	0.178	1.4×10^4	−513 ± 32
324-051	−0.050 ± 0.400	0.839 ± 0.167	23	0.378	6.5×10^4	−266 ± 38
314-037	0.350 ± 0.250	0.509 ± 0.590	22	0.268	2.3×10^4	−484 ± 54
222-277	0.300 ± 0.600	0.719 ± 0.716	22	0.346	4.5×10^4	−320 ± 55
292-010	−1.350 ± 0.550	2.748 ± 1.151	22	1.110	1.7×10^5	−392 ± 56

Notes.—Matched using a χ^2 minimization of our measured Lick indices for the young M31 clusters. The value N refers to the number of Lick indices utilized in the fitting procedure. Remeasured velocities for the clusters using new templates are also given.

stars. As such, it reflects the solar-neighborhood abundance pattern. This creates an abundance ratio bias that is implicit in stellar population models that employ empirical stellar libraries (Trager et al. 2000; Thomas et al. 2003; Proctor & Sansom 2002). For very young systems correcting for this bias is highly uncertain, and therefore we make no correction to the BC03 models. This should not introduce serious errors in our derived abundances near to solar metallicity (Proctor et al. 2004).

For each cluster, we perform a χ^2 fit of all our measured indices to each combination of age and metallicity in the BC03 models. The age and metallicity of the model that is best found to fit these data are then adopted as the best age and metallicity estimate of the particular cluster in question. For detailed discussions of the method applied to galaxy spectra see Proctor & Sansom (2002) and Proctor et al. (2004). The results of our χ^2 analysis are given in Table 8, and we show the "age-metallicity" relation for these clusters in Figure 12. For comparison, we have also performed the same analysis for a subset of the Beasley et al. (2002b) LMC clusters.

The majority of the ages derived from the BC03 models are consistent with those obtained from the LMC cluster templates. However, the BC03 models do generally predict older ages than these templates. This is consistent with the idea that the LMC templates are somewhat more metal-poor than the young M31 clusters. For Hubble V, we obtain an age of 0.51 ± 0.59 Gyr, which is consistent with previous studies (Da Costa & Mould 1988; Lee 1996). Figure 12 shows that, with the exception of 292-010, all of the young clusters are less than 1 Gyr old and are very close to solar metallicity. Cluster 292-010 appears to be closer to 3 Gyr old and is also somewhat more metal-poor. We conclude that our age determinations are in reasonable accord with the LMC templates, and henceforth we adopt the age and metallicity estimates for the young clusters based on the BC03 models, which are given in Table 8. We are now in a position to estimate the masses of the clusters.

We have dereddened the V-band apparent magnitudes of the clusters using the mean reddening, $E(B-V) = 0.22$, derived by Barmby et al. (2000) and adopting $R_V = 3.2$ (Cardelli et al. 1989). Assuming a distance modulus to M31 of $\mu = 24.47$ (Holland 1998; Stanek & Garnavich 1998), we obtain absolute magnitudes and hence total V-band luminosities for the clusters. The M/L_V ratios for the clusters come from BC03, based on our BC03 age determinations. This has the benefit of adding internal consistency to our calculations. In Table 8 we list the adopted M/L_V ratios and estimated masses for the young M31 clusters. Estimating the uncertainties in our mass determinations is difficult, as a major contribution to the error budget is the unknown reddening in the disk of M31. An increase in our adopted mean reddening by a factor of 2 [$E(B-V) = 0.44$] would roughly increase our mass estimate by the same factor. An adopted factor of 2 uncertainty in the values given in Table 8 is not unreasonable. The Chabrier (2003) IMF used in the BC03 models predicts that aging these clusters to ~13 Gyr will result in their fading by up to 4 mag. Given their current absolute magnitude range of $-8.57 \leq M_V \leq -7.24$, this will result in clusters with $-4.57 \leq M_V \leq -3.24$, which is some 4 mag fainter than the peak of the Galactic GC luminosity function.

A further consideration in this mass calculation is the effect of dynamical evolution, both internal and external to the clusters (e.g., Fall & Zhang 2001). Several effects are expected

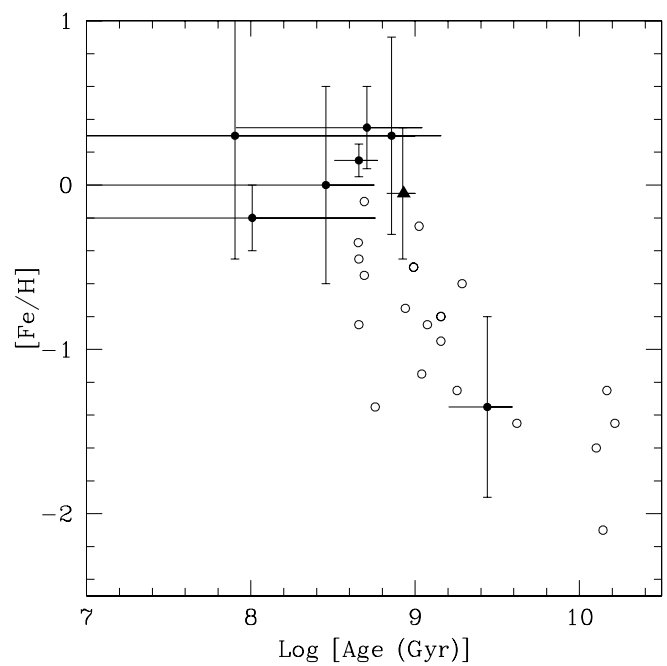

Fig. 12.—Ages and metallicities for the young M31 clusters (*filled circles with error bars*) and LMC clusters from Beasley et al. (2002b; *open circles* [error bars omitted for clarity]) based on the predictions of the Bruzual & Charlot (2003) stellar population models. The position of Hubble V, the NGC 205 cluster, is marked with a filled triangle.

to occur on different timescales, which will act to lower the cluster masses. For ages $\leq 10^8$ yr, stellar winds and supernovae will remove some $\sim$30% of the initial mass from a cluster, whereas for clusters older than this, two-body relaxation, bulge and/or disk shocking, and dynamical friction will all act on the clusters to varying degrees. The survival of Galactic *open* clusters (OCs) at a given mass depends crucially upon their linear size (Wielen 1971). Massive but small clusters feel the effects of dynamical relaxation most strongly, whereas more extended clusters are more susceptible to the effects of the galactic tidal field. For the M31 clusters in question, with masses $\sim 10^4\ M_\odot$, we expect two-body relaxation to be the primary source of mass evolution (Gnedin & Ostriker 1997). Obtaining structural parameters for these clusters will shed light on this important issue. Suffice it to say that our mass estimates do not correct for any dynamical evolution.

The cluster masses and "faded" absolute magnitudes we derive are relatively modest in GC terms. Some 90% of the Galactic GC system have masses $\geq 1 \times 10^5\ M_\odot$. The only cluster in the sample that lies in this GC mass regime is the slightly older, more metal-poor 292-010, which lies out of the plane of the disk (see below). For reference, one of the least massive GCs known in the Galaxy is AM-4, which has an absolute magnitude $M_V = -1.24$. Assuming $M/L_V = 2$ for an old stellar population, we obtain a mass of $8.4 \times 10^3\ M_\odot$ for this cluster.

An important question here is whether these are actually young GCs, OCs, or lie somewhere else in the mass spectrum of star clusters. After Larsen & Richtler (1999), in Figure 13 we plot the young M31 clusters in the M_V-age plane compared to the Galactic OC catalog of Lyngå (1987) and the young, massive clusters (YMCs) identified in a sample of nearby spiral galaxies by Larsen & Richtler (1999).

The comparison between the young M31 clusters, the OCs, and the YMCs is not strictly fair for two reasons. First, ages are derived for these latter two cluster types using integrated colors, whereas the M31 clusters have spectroscopically derived ages. Secondly, and perhaps more importantly, the selection functions of the three cluster types are very different. However, Figure 13 is revealing. The Galactic OCs from Lyngå (1987) are rather well bounded by the BC03 models for $M = 10^4\ M_\odot$ at solar metallicity. Very few are found to lie above this mass for the Chabrier IMF. With the exception of 327-053, all the M31 clusters are well separated from the upper envelope of the Galactic OCs. In fact, the M31 clusters roughly cover the mass range of the YMCs of Larsen & Richtler (1999), although they are somewhat older. This is probably not a real effect but reflects a bias in the Larsen & Richtler sample in that they preferentially obtained data for the bright end of the YMC luminosity function, which are intrinsically younger YMCs.

Also in Figure 13 we show the position of a GC at the turnover of the globular cluster luminosity function (GCLF; $M_V = -7.4$), with an observed dispersion of 1.2 mag. As the young M31 clusters fade and follow the locus of the models, they occupy an area slightly below this region, between the GCs and OCs. Therefore, at present, we cannot say for certain whether we are seeing massive OCs or relatively low-mass GCs. High-resolution imaging and dynamical mass estimates will distinguish between these two possibilities.

With the exceptions of Hubble V (an NGC 205 cluster) and 292-010, all the clusters lie at or around solar metallicities, are less than 1 Gyr old, and are projected onto the disk of M31

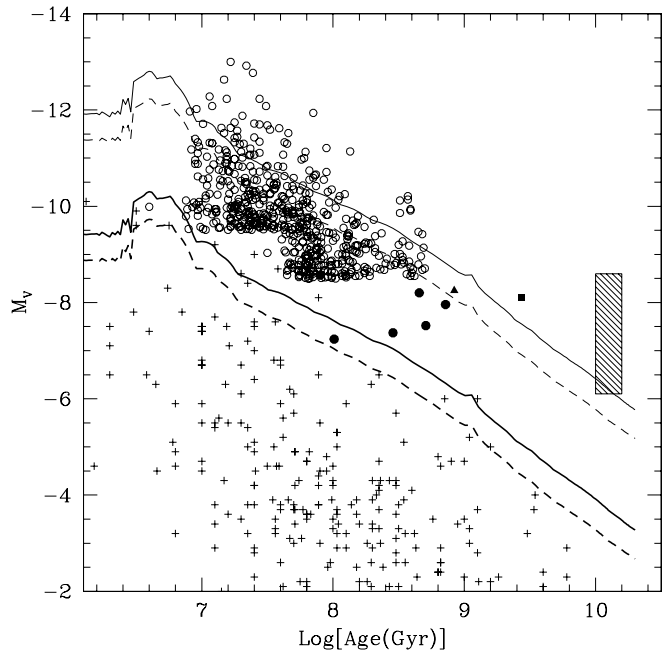

FIG. 13.—Comparison of the young M31 clusters (*filled symbols*), open cluster data from Lyngå (1987; *plus signs*) and young massive cluster data from Larsen & Richtler (1999; *open circles*) in the M_V–log(age) plane. Hubble V in NGC 205 is marked as a triangle; 292-010, which lies out of the plane of the disk, is marked as a square. The hatched region denotes the area occupied by Milky Way GCs with mean $M_V = -7.4$ and a dispersion of 1.2 mag. Lines represent the predictions of the Bruzual & Charlot (2003) models for the fading with age of a cluster at masses $M = 10^4\ M_\odot$ (*thick lines*) and $10^5\ M_\odot$ (*thin lines*) at solar metallicity. Dashed and solid lines represent Salpeter and Chabrier IMFs, respectively.

(Fig. 1). Cluster 292-010 lies $\sim$10 kpc to the southwest of NGC 205, approximately 7 kpc away from the disk. Are we, in fact, looking at a disk system of young clusters in M31? We first need to redetermine the velocities of these young clusters prior to looking at their kinematics, since their broad Balmer lines lead to serious systematic errors when their spectra are cross-correlated against classical G and K templates (Barmby et al. 2000). This possibility may afflict part of the Perrett et al. (2002) sample. We derive new velocities for the young clusters by cross-correlation with a series of A and F star templates from the STELIB spectral library. These new velocities and their respective uncertainties are given in Table 8. In Figure 14, we plot the rotation curve of the six young clusters compared to the rotation curve derived from H II regions of M31 by Rubin & Ford (1970) and the H I curve of Kent (1989).

The clusters show signs of rotating in the same sense as, and with a similar amplitude to, these H I and H II data. Unfortunately, the small sample and low resolution of our spectra are unsuitable for a detailed analysis of this issue. Interestingly, on the basis of accurate velocities for $\sim$200 M31 GCs (Perrett et al. 2002), Morrison et al. (2004) have suggested the existence of a *thin* disk system of GCs in M31. This is in contrast to the Milky Way, which seems to have no such system. Moreover, these authors showed that, based on the Perrett et al. metallicities, the clusters cover a metallicity range $-2.0 \leq [\mathrm{Fe/H}] \leq 0$. This is significantly more metal-poor than the Milky Way stellar thin disk. Morrison et al. (2004) argued that, although they had no secure age estimates for these disk clusters, the fact that the disk clusters extend down to such low metallicities was indicative that the thin disk of M31 was likely to be old ($\sim$10 Gyr).

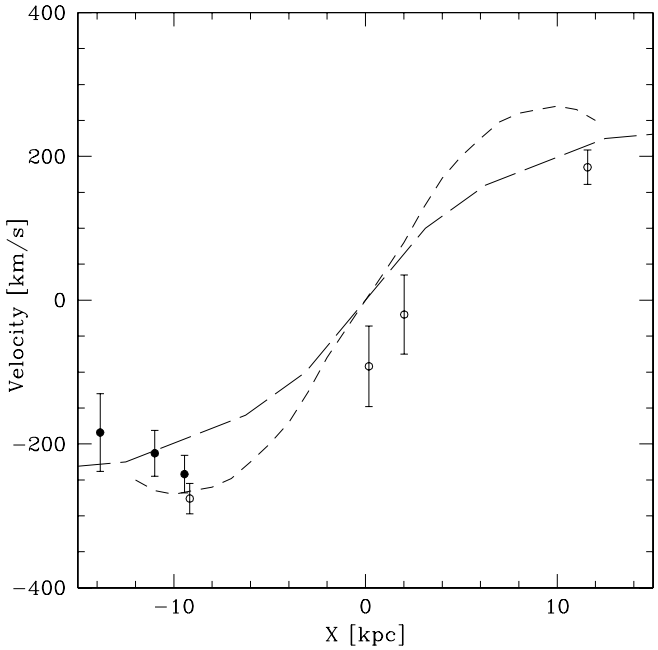

Fig. 14.—Velocity vs. the projected distance along the major axis of M31. The six young clusters are compared to the rotation of M31 H II regions from Rubin & Ford (1970; *short-dashed lines*) and the H I rotation curve of Kent (1989; *long-dashed lines*), assuming the same distance modulus. The H I and H II data have been folded on the *x*- and *y*-axes and extrapolated interior to 3 kpc. All velocities have been corrected to the M31 rest frame by +300 km s^{-1}. Filled symbols represent the three clusters identified as possessing thin disk kinematics by Morrison et al. (2004). The young clusters show evidence of rotation similar to that of M31's gas disk.

Four of the six disk clusters in our sample are included in the Morrison et al. (2004) study, namely, 314-037, 321-046, 327-053 and 380-313. Of these four, three have residuals from a disk model $\leq$0.75, corresponding to thin-disk kinematics (see Morrison et al. 2004 for the precise definitions): 314-037 (0.57), 321-046 (−0.05), and 327-053 (0.25). These are consistent with their definition of belonging to a thin disk population, and indeed these clusters lie near the rotation curves shown in Figure 14. However, rather than being old, metal-poor disk clusters as suggested by Morrison et al. (2004), we find that these clusters are young and at approximately solar metallicity. We suggest that the age-metallicity degeneracy and the lack of Balmer lines in the Perrett et al. (2002) spectra led these authors to conclude incorrectly that these were metal-poor rather than young objects. A full census of the ages of these disk clusters is required to investigate this point.

6. DISCUSSION

There appear to be at least two striking differences between the M31 GC system and that of the Milky Way.

6.1. *Nitrogen Enhancement*

Since the work of Burstein et al. (1984), it has been known that CN in the integrated spectra of M31 GCs is enhanced relative to Milky Way GCs. We have shown that this remains true for GCs in the range $-1.5 \leq [\mathrm{Fe/H}] \leq -0.3$ (the metallicity range of the Milky Way GCs in our sample). Moreover, both the M31 and Milky Way GCs are enhanced in CN when compared to elliptical galaxies, which themselves show differences when divided into field and cluster samples (Sánchez-Blázquez et al. 2003). The very existence of CN variations suggests that N is the main culprit, since C is expected to be effectively absorbed into the CO molecule. This is supported by observations of the NH feature at 3360 Å (Ponder et al. 1998; Li & Burstein 2003). The behavior of C is less clear, although from the point of view of stellar evolution C is expected to be destroyed in favor of N if the sum of C + N + O is preserved. A better understanding of the behavior of C and O in GCs may benefit from a comprehensive study of the CO feature at 2.3 μm (e.g., Davidge 1990).

Varying CN enhancements in the *integrated* spectra of Galactic and M31 clusters is particularly interesting when one considers the CN variations known to exist between stars in individual Galactic GCs. The best-documented case is that of 47 Tucanae. Norris & Freeman (1979) found that the giants in this cluster exhibited CN-strong and CN-weak bimodality from the CN molecular band at 4150 Å. This bimodality has since been observed to several magnitudes below the main-sequence turnoff in Galactic GCs. CN and CH also seem to be anticorrelated, as expected from the CNO cycle (e.g., Cannon et al. 1998; Gratton et al. 2001; Briley et al. 2002, 2004; Harbeck et al. 2003). Although no such studies exist for the much more distant M31 GCs, Tripicco (1989) and Tripicco & Bell (1992) showed that, on the basis of near-UV integrated spectroscopy and synthetic spectra, CN enhancement in the M31 GCs likely arises from CN-strong giants *and* CN-strong dwarfs. Thus, the luminosity dependence of CN appears to exist in M31 GCs as well as Milky Way clusters.

As discussed comprehensively by Cannon et al. (1998) and summarized by Harbeck et al. (2003), three scenarios have been discussed to explain these puzzling chemical inhomogeneities: internal evolution of GC stars, GC self-pollution from evolved stars, and primordial differences or GC self-enrichment.

Both the internal evolution and GC self-pollution scenarios have difficulty explaining the observed bimodality in CN in general, as well as its existence well below the main-sequence turnoff in GCs. CNO variations are expected to occur on the giant branch from standard mixing theory, where the convective envelope reaches its closest penetration to the CNO burning shell. However, this is not expected in stars well below the main-sequence turnoff, which are not expected to undergo deep mixing (Renzini & Voli 1981). Self-pollution from asymptotic giant branch stars are expected to eject CNO products through stellar winds, which may be deposited upon the rest of the stars in the cluster (Ventura et al. 2001). However, such accreted material is expected to be diluted in red giant branch stars that undergo deep mixing. This is generally not observed, except possibly in a few metal-poor GCs (Suntzeff 1981; Carbon et al. 1982).

The primordial scenario argues that the protoglobular clouds had a range of chemical compositions, and a collision between two such clouds may result in the observed bimodality if the gas remained unmixed prior to the onset of star formation. This picture is not unreasonable in an early protogalactic environment, where the cross-section of cloud-cloud collisions is expected to be high (Bekki et al. 2004). However, this scenario faces the constraint that the iron-peak elements show very little dispersion in individual GCs (e.g., Kraft 1994).

All of the M31 GCs in our sample have similar metallicities and luminosities to their Galactic counterparts and lie on the same fundamental plane (Barmby et al. 2002). These clusters are enhanced in CN with respect to the Milky Way GCs, which themselves show cluster-to-cluster variations (Cannon et al. 1998). It seems unlikely that internal evolution or self-pollution would operate preferentially in the M31 GCs but not in Milky

Way clusters, particularly since the M31 GC dwarfs are likely CN-strong (Tripicco & Bell 1992; Li & Burstein 2003). Unless there are significant age differences between the Milky Way GCs and all the M31 clusters in our sample (which we have not observed; Paper II), it seems highly likely that the source of the CN enhancement was external to the M31 cluster system.

Although highly speculative, we are forced to conclude that the nitrogen enhancement in M31 GCs must be primordial in origin. The M31 protoglobular clouds were presumably enriched in nitrogen at some early epoch, whereas the protoglobular clouds of the Milky Way GCs were not. Much of the remaining nitrogen-rich material must have become incorporated into the bulk of the galaxy itself, although the M31 bulge shows significantly lower CN than the M31 GCs. With the advent of larger aperture telescopes, fine abundance analysis of individual halo stars in M31 would be extremely interesting in this regard.

6.2. *Young Disk Clusters*

Six of the young clusters in our sample appear to be disk clusters. They are projected on to the M31 disk, appear to rotate with the H I gas, and have approximately solar metallicities. Interestingly, one nondisk cluster appears to be somewhat older ($\sim$3 Gyr) and lies approximately 7 kpc away from the plane of the disk. On the basis of our mass estimates, it is presently not clear whether these objects are true GCs. Provided that they survive the dual effects of the tidal field of M31 and two-body relaxation, they may possibly evolve to populate the fainter end of the GCLF or populate the bright end of the open cluster luminosity function.

Are these clusters unusual? The work of Larsen & Richtler (1999, 2000) highlighted the fact that YMCs are actually a common feature of local spiral galaxies. The presence of young disk clusters in M31 is therefore not surprising. On the basis of a sample of 31 nearby spiral galaxies, Larsen & Richtler (2000) found a correlation between the specific U-band YMC luminosity, $T_L(U)$, and the star formation rate (SFR) of the galaxies as traced by the far infrared luminosity of the host galaxy.

It is interesting to ask the question: where does M31 lie on this relation? Using equation (7) of Larsen & Richtler (2000), based on the far-infrared luminosity of M31, we obtain a normalized SFR for this galaxy of $1.9 \times 10^{-4}\ M_{\odot}\ \mathrm{yr}^{-1}\ \mathrm{kpc}^{-2}$. Assuming that all the metal-poor ($[\mathrm{Fe/H}] < -1.0$) disk clusters in the Morrison et al. (2004) sample are young clusters and adopting a mean U-band absolute magnitude of $\langle M_U \rangle = -6.7$ (Barmby et al. 2000), we obtain $T_L(U) = 0.02$. Clearly the sample of M31 disk clusters is not complete, but these values suggest that M31 lies on the Larsen & Richtler (2000) relation and in the reasonably low-SFR, low-$T_L(U)$ regime (see Figs. 3 and 5 of Larsen & Richtler 2000). This lends support to the idea that these objects are not open clusters in M31 and may represent the precursors of true thin disk GCs.

A system of young disk GCs is not seen in the Milky Way, and if M31 is truly forming disk GCs, then this has important implications for galaxy formation theories. GCs are thought to trace the early episodes of the collapse of their host galaxy (e.g., Searle & Zinn 1978; Forbes et al. 1997), as well as later accretion (Côté et al. 1998) and galaxy merging (Ashman & Zepf 1992). Our results suggest that GCs may also trace the buildup of galaxy disks, both at the present epoch and at higher redshifts. Indeed, the very existence of such disk clusters is expected on the basis that disks are where the majority of present-day star formation occurs. Recent efforts to simulate GC formation in the cold dark matter paradigm also identify that a large fraction of GCs are expected to form in disklike structures at high redshift (Beasley et al. 2002a; Kravtsov & Gnedin 2003).

Morrison et al. (2004) have recently argued for the existence of a thin disk in M31 on the basis of GC kinematics, which extends down to $[\mathrm{Fe/H}] \sim -2.0$. Such an old disk is perhaps not unexpected from a theoretical standpoint, if it can avoid disruptive merging in the dense, early universe (Baugh et al. 1996; Abadi et al. 2003). The observational constraints in this regard are not so clear, since the stellar thin disk of the Milky Way is the only such disk heretofore known to exist. However, in general, spiral stellar disks are thought to be metal-rich, if not relatively young (Bell & de Jong 2000).

We have found that, rather than being old and metal-poor, the M31 disk clusters are in fact young and metal-rich. A larger census of these young disk clusters is required to see if they populate the entire low-metallicity sample of Morrison et al. (2004); however, the implication is clear. On the basis of our cluster data, the thin disk identified by Morrison et al. (2004) may in fact be significantly younger than 10 Gyr (possibly as young as the oldest $\sim$1 Gyr cluster), with a metallicity not too dissimilar to that of the Milky Way disk.

Brown et al. (2003) recently reported the presence of a significant intermediate-aged (6–8 Gyr) and metal-rich ($[\mathrm{Fe/H}] > -0.5$) population of stars in a minor-axis halo field of M31, based on deep *HST*/ACS imaging. These authors suggested that M31 may have undergone a nearly equal-mass merger 6–8 Gyr in the past. The presence of an old thin disk as identified by Morrison et al. (2004) effectively ruled out such a scenario, since any disk would be disrupted in such an event. With the identification that the thin disk of M31 may be as young as $\sim$1 Gyr, the suggestion by Brown et al. (2003) becomes more tenable.

Based on the evidence of enhanced N and a disk population of possible GCs in M31, it appears then that not all GC systems of spiral galaxies are born equal. Both the initial chemical enrichment and star formation (possibly merger history) of these two galaxies have differed significantly. Future work required includes a full census of the young star clusters in M31, secure mass determinations of these clusters, further near-UV and IR spectroscopy to understand the role of N and C, respectively, in GCs, and extensive spectroscopic and near-UV imaging surveys of a greater number of local spiral galaxies.

We thank Javier Cenarro, Michael Pierce, and Michael Rich for useful comments and suggestions on the paper and Chris Flynn and Brad Gibson for early discussions regarding this work. We also thank P. Sánchez-Blázquez for supplying her thesis data ahead of full publication and Søren Larsen for providing the YMC data. We are also very grateful to Judy Cohen and John Blakeslee for supplying the LRIS Galactic GC spectra in digital form. Funding support comes from NSF grant AST-0206139. The data presented herein were obtained at the W. M. Keck Observatory, which is operated as a scientific partnership among the California Institute of Technology, the University of California, and the National Aeronautics and Space Administration. The Observatory was made possible by the generous financial support of the W. M. Keck Foundation. This research has made use of the NASA/IPAC Extragalactic Database (NED), which is operated by the Jet Propulsion Laboratory, Caltech, under contract with the National Aeronautics and Space Administration.

REFERENCES

Abadi, M. G., Navarro, J. F., Steinmetz, M., & Eke, V. R. 2003, ApJ, 591, 499
Ashman, K. M., & Zepf, S. E. 1992, ApJ, 384, 50
Barmby, P., Holland, S., & Huchra, J. P. 2002, AJ, 123, 1937
Barmby, P., Huchra, J. P., Brodie, J. P., Forbes, D. A., Schroder, L. L., & Grillmair, C. J. 2000, AJ, 119, 727
Battistini, P., Bonoli, F., Braccesi, A., Federici, L., Fusi Pecci, F., Marano, B., & Borngen, F. 1987, A&AS, 67, 447
Battistini, P., Bonoli, F., Braccesi, A., Fusi Pecci, F., Malagnini, M. L., & Marano, B. 1980, A&AS, 42, 357
Battistini, P. L., Bonoli, F., Casavecchia, M., Ciotti, L., Federici, L., & Fusi Pecci, F. 1993, A&A, 272, 77
Baugh, C. M., Cole, S., & Frenk, C. S. 1996, MNRAS, 283, 1361
Beasley, M. A., Baugh, C. M., Forbes, D. A., Sharples, R. M., & Frenk, C. S. 2002a, MNRAS, 333, 383
Beasley, M. A., Forbes, D. A., Brodie, J. P., & Kissler-Patig, M. 2004a, MNRAS, 347, 1150
Beasley, M. A., Hoyle, F., & Sharples, R. M. 2002b, MNRAS, 336, 168
Beasley, M. A., Sharples, R. M., Bridges, T. J., Hanes, D. A., Zepf, S. E., Ashman, K. M., & Geisler, D. 2000, MNRAS, 318, 1249
Beasley, M. A., et al. 2004b, in preparation (Paper II)
Bekki, K., Beasley, M. A., Forbes, D. A., & Couch, W. J. 2004, ApJ, 602, 730
Bell, E. F., & de Jong, R. S. 2000, MNRAS, 312, 497
Bellazzini, M., Cacciari, C., Federici, L., Fusi Pecci, F., & Rich, M. 2003, A&A, 405, 867
Bica, E., Claria, J. J., & Dottori, H. 1992, AJ, 103, 1859
Briley, M. M., Cohen, J. G., & Stetson, P. B. 2002, ApJ, 579, L17
———. 2004, AJ, 127, 1579
Brodie, J. P., & Huchra, J. P. 1990, ApJ, 362, 503
———. 1991, ApJ, 379, 157
Brook, C. B., Kawata, D., Gibson, B. K., & Flynn, C. 2003, ApJ, 585, L125
Brown, T. M., Ferguson, H. C., Smith, E., Kimble, R. A., Sweigart, A. V., Renzini, A., Rich, R. M., & VandenBerg, D. A. 2003, ApJ, 592, L17
Bruzual, G., & Charlot, S. 2003, MNRAS, 344, 1000 (BC03)
Burstein, D., Faber, S. M., Gaskell, C. M., & Krumm, N. 1984, ApJ, 287, 586
Cannon, R. D., Croke, B. F. W., Bell, R. A., Hesser, J. E., & Stathakis, R. A. 1998, MNRAS, 298, 601
Carbon, D. F., Romanishin, W., Langer, G. E., Butler, D., Kemper, E., Trefzger, C. F., Kraft, R. P., & Suntzeff, N. B. 1982, ApJS, 49, 207
Cardelli, J. A., Clayton, G. C., & Mathis, J. S. 1989, ApJ, 345, 245
Cardiel, N., Gorgas, J., Cenarro, J., & Gonzalez, J. J. 1998, A&AS, 127, 597
Chabrier, G. 2003, PASP, 115, 763
Chandar, R., Bianchi, L., & Ford, H. C. 1999, ApJS, 122, 431
Chandar, R., Whitmore, B., & Lee, M. G. 2004, ApJ, 611, 220
Cohen, J. G. 1982, ApJ, 258, 143
Cohen, J. G., Blakeslee, J. P., & Ryzhov, A. 1998, ApJ, 496, 808 (CBR98)
Cohen, J. G., Briley, M. M., & Stetson, P. B. 2002, AJ, 123, 2525
Côté, P. 1999, AJ, 118, 406
Côté, P., Marzke, R. O., & West, M. J. 1998, ApJ, 501, 554
Côté, P., Marzke, R. O., West, M. J., & Minniti, D. 2000a, ApJ, 533, 869
Côté, P., Mateo, M., Sargent, W. L. W., & Olszewski, E. W. 2000b, ApJ, 537, L91
Crampton, D., Cowley, A. P., Schade, D., & Chayer, P. 1985, ApJ, 288, 494
Da Costa, G. S., & Mould, J. R. 1988, ApJ, 334, 159
Davidge, T. J. 1990, ApJ, 351, L37
Elson, R. A. W., Fall, S. M., & Freeman, K. C. 1987, ApJ, 323, 54
Fall, S. M., & Zhang, Q. 2001, ApJ, 561, 751
Forbes, D. A., Brodie, J. P., & Grillmair, C. J. 1997, AJ, 113, 1652
Forbes, D. A., Brodie, J. P., & Larsen, S. S. 2001, ApJ, 556, L83
Forbes, D. A., Strader, J., & Brodie, J. P. 2004, AJ, 127, 3394
Freeman, K., & Bland-Hawthorn, J. 2002, ARA&A, 40, 487
Frenk, C. S., & White, S. D. M. 1982, MNRAS, 198, 173
Geisler, D., Piatti, A. E., Bica, E., & Clariá, J. J. 2003, MNRAS, 341, 771
Girardi, L., Chiosi, C., Bertelli, G., & Bressan, A. 1995, A&A, 298, 87
Gnedin, O. Y., & Ostriker, J. P. 1997, ApJ, 474, 223
González, J. J. 1993, Ph.D. thesis, Univ. California, Santa Cruz
Gottesman, S. T., Hunter, J. H., & Boonyasait, V. 2002, MNRAS, 337, 34
Goudfrooij, P., Strader, J., Brenneman, L., Kissler-Patig, M., Minniti, D., & Edwin Huizinga, J. 2003, MNRAS, 343, 665
Gratton, R. G., et al. 2001, A&A, 369, 87
Harbeck, D., Smith, G. H., & Grebel, E. K. 2003, AJ, 125, 197
Hodge, P. W., & Wright, F. W. 1967, The Large Magellanic Cloud (Washington: Smithsonian Press)
Holland, S. 1998, AJ, 115, 1916
Holland, S., Fahlman, G. G., & Richer, H. B. 1996, AJ, 112, 1035
Huchra, J. P., Brodie, J. P., & Kent, S. M. 1991, ApJ, 370, 495
Jensen, J., Mould, J., & Reid, N. 1988, ApJS, 67, 77
Kent, S. M. 1989, AJ, 97, 1614
Kim, S. C., Lee, M. G., Geisler, D., Sarajedini, A., Armandroff, T. E., & da Costa, G. S. 2002, in IAU Symp. 207, Extragalactic Star Clusters, ed. E. Grebel, D. Geisler, & D. Minniti (San Francisco: ASP), 174
King, I. R. 1966, AJ, 71, 64
Kraft, R. P. 1994, PASP, 106, 553
Kravtsov, A. V., & Gnedin, O. Y. 2003, ApJ, submitted (astro-ph/0305199)
Kuntschner, H., Ziegler, B. L., Sharples, R. M., Worthey, G., & Fricke, K. J. 2002, A&A, 395, 761
Larsen, S. S., & Brodie, J. P. 2002, AJ, 123, 1488
Larsen, S. S., & Richtler, T. 1999, A&A, 345, 59
———. 2000, A&A, 354, 836
Le Borgne, J.-F., et al. 2003, A&A, 402, 433
Lee, H., Yoon, S., & Lee, Y. 2000, AJ, 120, 998
Lee, M. G. 1996, AJ, 112, 1438
Leonardi, A. J., & Rose, J. A. 2003, AJ, 126, 1811
Li, Y., & Burstein, D. 2003, ApJ, 598, L103
Lyngå, G. 1987, A Computer Readable Catalogue of Open Cluster Data (5th ed.; Strasbourg: CDS)
Madore, B. F., & Arp, H. C. 1982, PASP, 94, 40
Martin, N. F., Ibata, R. A., Bellazzini, M., Irwin, M. J., Lewis, G. F., & Dehnen, W. 2004, MNRAS, 348, 12
Minitti, D. 1995, AJ, 109, 1663
Morrison, H. L., Harding, P., Perrett, K., & Hurley-Keller, D. 2004, ApJ, 603, 87
Norris, J., & Freeman, K. C. 1979, ApJ, 230, L179
Oke, J. B. 1990, AJ, 99, 1621
Oke, J. B., et al. 1995, PASP, 107, 375
Olsen, K. A. G., Hodge, P. W., Mateo, M., Olszewski, E. W., Schommer, R. A., Suntzeff, N. B., & Walker, A. R. 1998, MNRAS, 300, 665
Olsen, K. A. G., Miller, B. W., Suntzeff, N. B., Schommer, R. A., & Bright, J. 2004, AJ, 127, 2674
Olszewski, E. W., Schommer, R. A., Suntzeff, N. B., & Harris, H. C. 1991, AJ, 101, 515
Perrett, K. M., Bridges, T. J., Hanes, D. A., Irwin, M. J., Brodie, J. P., Carter, D., Huchra, J. P., & Watson, F. G. 2002, AJ, 123, 2490
Peterson, R. 1989, in Dynamics of Dense Stellar Systems, ed. D. Merritt (Cambridge: Cambridge Univ. Press), 161
Piatti, A. E., Geisler, D., Bica, E., & Clariá, J. J. 2003, MNRAS, 343, 851
Ponder, J. M., et al. 1998, AJ, 116, 2297
Proctor, R. N., Forbes, D. A., Hau, G. K. T., Beasley, M. A., De Silva, G. M., Contreras, R., & Terlevich, A. I. 2004, MNRAS, 349, 1381
Proctor, R. N., & Sansom, A. E. 2002, MNRAS, 333, 517
Puzia, T. H., Saglia, R. P., Kissler-Patig, M., Maraston, C., Greggio, L., Renzini, A., & Ortolani, S. 2002, A&A, 395, 45 (P02)
Rabin, D. M. 1981, Ph.D. thesis, Caltech
Renzini, A., & Voli, M. 1981, A&A, 94, 175
Rhode, K. L. 2003, Ph.D. thesis, Yale Univ.
Rich, R. M., Reitzel, D. B., Guhathakurta, P., Gebhardt, K., & Ho, L. C. 2004, AJ, 127, 2139
Rose, J. A. 1985, AJ, 90, 1927
Rosenberg, A., Saviane, I., Piotto, G., & Aparicio, A. 1999, AJ, 118, 2306
Rubin, V. C., & Ford, W. K. J. 1970, ApJ, 159, 379
Salaris, M., & Weiss, A. 2002, A&A, 388, 492
Sánchez-Blázquez, P., Gorgas, J., Cardiel, N., Cenarro, J., & González, J. J. 2003, ApJ, 590, L91
Sargent, W. L. W., Kowal, C. T., Hartwick, F. D. A., & van den Bergh, S. 1977, AJ, 82, 947
Schaller, G., Schaerer, D., Meynet, G., & Maeder, A. 1992, A&AS, 96, 269
Schroder, L. L., Brodie, J. P., Kissler-Patig, M., Huchra, J. P., & Phillips, A. C. 2002, AJ, 123, 2473
Searle, L., Wilkinson, A., & Bagnuolo, W. G. 1980, ApJ, 239, 803 (SWB80)
Searle, L., & Zinn, R. 1978, ApJ, 225, 357
Spinrad, H., & Schweizer, F. 1972, ApJ, 171, 403
Stanek, K. Z., & Garnavich, P. M. 1998, ApJ, 503, L131
Strader, J., Brodie, J. P., & Forbes, D. A. 2004, AJ, 127, 3431
Suntzeff, N. B. 1981, ApJS, 47, 1
Thomas, D., Maraston, C., & Bender, R. 2003, MNRAS, 339, 897
Trager, S. C. 2004, in Origin and Evolution of the Elements, ed. A. McWilliam & M. Rauch (Cambridge: Cambridge Univ. Press), 391
Trager, S. C., Faber, S. M., Worthey, G., & González, J. J. 2000, AJ, 120, 165
Trager, S. C., Worthey, G., Faber, S. M., Burstein, D., & González, J. J. 1998, ApJS, 116, 1
Tripicco, M. J. 1989, AJ, 97, 735
Tripicco, M. 1993, in ASP Conf. Ser. 48, The Globular Cluster—Galaxy Connection, ed. G. H. Smith & J. P. Brodie (San Francisco: ASP), 432

Tripicco, M. J., & Bell, R. A. 1990, AJ, 99, 691
———. 1992, AJ, 103, 1285
van den Bergh, S. 1969, ApJS, 19, 145
———. 1975, ARA&A, 13, 217
———. 1999, A&A Rev., 9, 273
Vazdekis, A. 1999, ApJ, 513, 224
Ventura, P., D'Antona, F., Mazzitelli, I., & Gratton, R. 2001, ApJ, 550, L65
Wielen, R. 1971, A&A, 13, 309
Worthey, G., Faber, S. M., González, J. J., & Burstein, D. 1994, ApJS, 94, 687
Worthey, G., & Ottaviani, D. L. 1997, ApJS, 111, 445
Zinn, R. 1985, ApJ, 293, 424
Zinn, R., & West, M. 1984, ApJS, 55, 45